Morphogenic responses and biochemical alterations induced by the cover crop Urochloa ruziziensis and its component protodioscin in weed species

Journal Pre-proof

Morphogenic responses and biochemical alterations induced by the cover crop *Urochloa ruziziensis* and its component protodioscin in weed species

Paulo Vinicius Moreira da Costa Menezes, Adriano Antonio Silva, Márcio Shigueaki Mito, Gislaine Cristiane Mantovanelli, Gabriel Felipe Stulp, Ana Luiza Wagner, Rodrigo Polimeni Constantin, Débora Cristina Baldoqui, Raísa Gonçales Silva, Amanda Aparecida Oliveira do Carmo, Luíz Antonio de Souza, Rubem Silvério de Oliveira Junior, Fabrizio Araniti, Maria Rosa Abenavoli, Emy Luiza Ishii-Iwamoto

PII: S0981-9428(21)00353-3

DOI: https://doi.org/10.1016/j.plaphy.2021.06.040

Reference: PLAPHY 6833

To appear in: *Plant Physiology and Biochemistry*

Received Date: 3 April 2021

Revised Date: 30 May 2021

Accepted Date: 22 June 2021

Please cite this article as: P.V.M. da Costa Menezes, A.A. Silva, Má.Shigueaki. Mito, G.C. Mantovanelli, G.F. Stulp, A.L. Wagner, R.P. Constantin, Dé.Cristina. Baldoqui, Raí.Gonç. Silva, A.A. Oliveira do Carmo, Luí.Antonio. de Souza, Rubem.Silvé. de Oliveira Junior, F. Araniti, M.R. Abenavoli, E.L. Ishii-Iwamoto, Morphogenic responses and biochemical alterations induced by the cover crop *Urochloa ruziziensis* and its component protodioscin in weed species, *Plant Physiology et Biochemistry* (2021), doi: https://doi.org/10.1016/j.plaphy.2021.06.040.

AUTHOR CONTRIBUTIONS

Paulo Vinicius Moreira da Costa Menezes: designed and developed the experiments as part of his M.Sc.thesis, performed the analytic calculations, analysed the data, designed the figures and drafted the manuscript.

Rodrigo Polimeni Constantin: verified the biochemical methods and contributed to planning, supervision and interpretation of the experiments

Márcio Shigueaki Mito: verified the biochemical methods and contributed to planning, supervision and interpretation of the experiments

Gislaine Cristiane Mantovanelli: verified the biochemical methods and contributed to planning, supervision and interpretation of the experiments.

Gabriel Felipe Stulp: contributed to execution of the experiments.

Ana Luiza Wagner Zampieri: supported the optimization of enzymatic assay experiments.

Adriano Antonio Silva: developed the methodology for extraction and chemical identification of soluble constituents of *U. ruziziensis* straws.

Débora Cristina Baldoqui: supervised the analytical methods for extraction and chemical identification of soluble constituents of *U. ruziziensis* straws.

Luíz Antonio de Souza: conceived, planned and supported the experiments of morpho-anatomical analysis of the roots.

Amanda Aparecida Oliveira do Carmo: performed the experiments of morpho-anatomical analyzis of the roots.

Raísa Gonçales Silva: performed the experiments of morpho-anatomical analyzis of the roots.

Rubem Silvério de Oliveira Junior: contributed to the conception of the work, carried out the planting and obtaining of *U. ruziziensis* straw, and contributed to discussion of manuscript.

Maria Rosa Abenavoli: contributed to the interpretation and statistical analysis of the data and provided critical feedback for the manuscript.

Fabrizio Araniti: contributed to the interpretation and statistical analysis of the data and provided critical feedback for the manuscript.

Emy Luiza Ishii-Iwamoto: conceived the original idea, supervised the M.Sc.thesis of Paulo V. M. C. Menezes, analysed the data and wrote the manuscript with input from all authors.

Graphic abstract

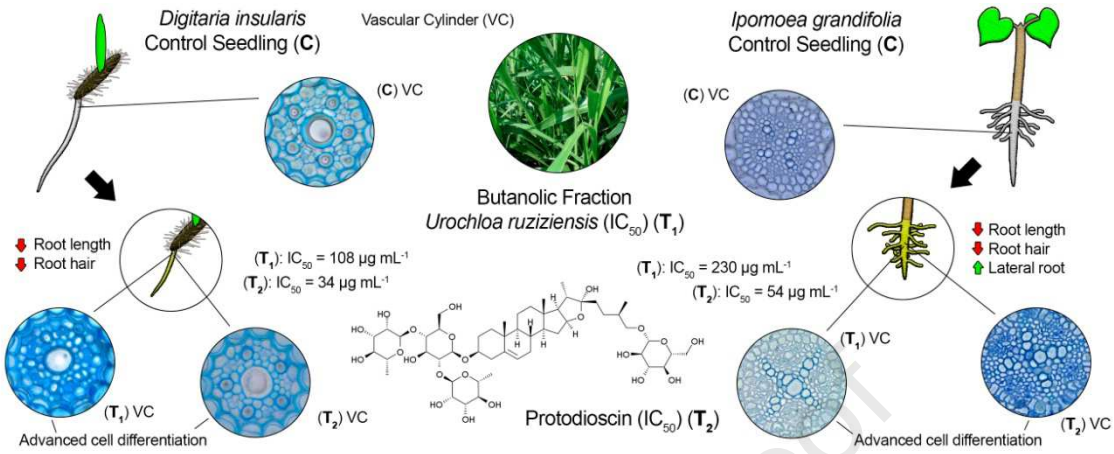

MORPHOGENIC RESPONSES AND BIOCHEMICAL ALTERATIONS INDUCED BY THE COVER CROP *Urochloa ruziziensis* AND ITS COMPONENT PROTODIOSCIN IN WEED SPECIES

Paulo Vinicius Moreira da Costa Menezes[1], Adriano Antonio Silva[2], Márcio Shigueaki Mito[1], Gislaine Cristiane Mantovanelli[1], Gabriel Felipe Stulp[1], Ana Luiza Wagner[1], Rodrigo Polimeni Constantin[1], Débora Cristina Baldoqui[3], Raísa Gonçales Silva[4], Amanda Aparecida Oliveira do Carmo[4], Luíz Antonio de Souza[4], Rubem Silvério de Oliveira Junior[5], Fabrizio Araniti[6], Maria Rosa Abenavoli[6], Emy Luiza Ishii-Iwamoto[1*]

[1]Department of Biochemistry, State University of Maringa, Brazil, [2]Center of Biological Sciences and Nature, Federal University of Acre, Rio Branco, Brazil, [3]Departament of Chemistry, State University of Maringa, Brazil, [4]Department of Biology, State University of Maringa, Brazil, [5]Department of Agronomy, State University of Maringa, Brazil, [6]Università Mediterranea di Reggio Calabria, Italy

*Corresponding author

E-mail: eliiwamoto@uem.br

Phone: +55-44-30114712

Affiliation: Laboratory of Biological Oxidations, Department of Biochemistry, State University of Maringá, 5790 Colombo Avenue, 87020900, Maringá, Paraná, Brazil.

ABSTRACT

Urochloa ruziziensis, a cover plant used in no-till systems, can suppress weeds in the field through their chemical compounds, but the mode of action of these compounds is still unknown. The present study aimed to investigate the effects of a saponin-rich butanolic extract from *U. ruziziensis* straw (Bf*Ur*) and one of its components, protodioscin on an eudicot *Ipomoea grandifolia* and a monocot *Digitaria insularis* weed. The anatomy and the morphology of the root systems and several parameters related to energy metabolism and antioxidant defense systems were examined. The IC_{50} values for the root growth inhibition by Bf*Ur* were 108 μg mL^{-1} in *D. insularis* and 230 μg mL^{-1} in *I. grandifolia*. The corresponding values for protodioscin were 34 μg mL^{-1} and 54 μg mL^{-1}. *I. grandifolia* exhibited higher ROS-induced peroxidative damage in its roots compared with *D. insularis*. In the roots of both weeds, the Bf*Ur* and protodioscin induced a reduction in the meristematic and elongation zones with a precocious appearance of lateral roots, particularly in *I. grandifolia*. The roots also exhibited features of advanced cell differentiation in the vascular cylinder. These alterations were similar to stress-induced morphologic responses (SIMRs), which are plant adaptive strategies to survive in the presence of toxicants. At concentrations above their IC_{50} values, the Bf*Ur* or protodioscin strongly inhibited the development of both weeds. Such findings demonstrated that *U. ruziziensis* mulches may contribute to the use of natural and renewable weed control tools.

Key words: respiration, plant development, saponin, antioxidant defense system, germination

ABBREVIATIONS:

ABA – Abscisic acid
AOX – Alternative oxidase
APX – Ascorbate peroxidase
AsA – Ascorbic acid
BfUr – Butanolic fraction of *Urochloa ruziziensis*
CAT – Catalase
COX – Ferrocytochrome-*c*:oxygenoxidoreductase
DCFDA – 2',7',-Dichlorofluorescin diacetate
DMSO – Dimethyl sulfoxide
GR – Glutathione reductase
HSD – Tukey's Honestly Significant Difference test
IAA – Indole-3-acetic acid

MDA – Malondialdehyde

NBT – Nitroblue tetrazolium

POD – Peroxidase

PPO - Polyphenol oxidase

PVP – Polyvinylpyrrolidone

ROS – Reactive oxygen species

SIMRs – Stress-induced morphogenic responses

SOD – Superoxide dismutase

TBA – Thiobarbituric acid

TCA – Trichloroacetic acid

1. INTRODUCTION

Cover plants used in no-tillage cropping systems contribute, through chemical compound production, to suppressing weed emergence, minimizing the negative impacts of excessive synthetic herbicide application. Evaluating nine cover treatments for weed suppression in no-tillage soybean production systems, São Miguel et al. (2018) verified that the cropping systems with *U. ruziziensis* promotes a lower incidence of weeds in most situations and species evaluated. Our previous work conducted in greenhouse supported the evidence that straw from *U. ruziziensis* reduces the emergence of weeds through chemical effects (Oliveira Jr et al., 2014). The inhibition of *Euphorbia heterophylla* and *Bidens pilosa* seedling growth was observed only when water percolated through the straws. We also have found that an aqueous fraction obtained from the straw of *U. ruziziensis* inhibits the initial growth of *Ipomoea grandifolia.* Many organic acids, including (*trans*)-aconitic acid were identified in this fraction (Foletto et al., 2012).

It has been also demonstrated that some species of *Urochloa spp.* (Poaceae) contain high levels of saponins, a class of compounds with a fairly large structural diversity (Brum et al., 2009; Lozano et al., 2017). The saponins may have steroid or triterpenoid structure, with one to three straight or branched sugar chains, which accounts for their diverse bioactivity (Podolak et al., 2010). The steroidal saponins protodioscin and protoneodioscin have been found in several species of the *Urochloa* genus (Brum et al., 2009; Nepomuceno et al., 2017; Silva, 2012). In particular, protodioscin has been suggested to be responsible for poisoning cases among cattle, goats, and sheep (Furlan et al., 2012). Its content is variable depending on the species; no protodioscin was detected in *Urochloa dictyoneura* or *Urochloa humidicola*, while toxic levels for animals (higher than 1% based on dry weight) were found in *Urochloa decumbens* and *Urochloa brizantha*, as well as hybrids of *U. brizantha*, *U. decumbens* and *U. ruziziensis* (Brum et al., 2009; Lozano et al., 2017).

Most studies concerning the activity of exogenous saponins on plants were related to crop protection against herbivores, insects, and fungi (Hussain et al., 2019; Mert-Türk, 2006). The direct influence of saponins on plant development has been poorly investigated, and studies have mainly focused on their effects on germination and biometric measurements of growth. Hoagland et al. (1996) examined the effects of several saponins and sapogenins on various weed and crop species and demonstrated that escin is the most active compound, reducing the emergence of many weeds and crop species when was applied to the soil. Furthermore, protodioscin isolated from *U. ruziziensis* inhibits the growth of *Glycine max* seedlings in laboratory conditions (Nepomuceno et al., 2017).

Despite the reports on the phytotoxicity of some saponins, their mechanisms of action have not been yet extensively studied. Due to their steroidal or triterpenoid structures, an interference with the action of steroidal phytohormones was investigated by Tsurumi et al. (2000). They demonstrated that the saponin chromosaponin I exerts an effect similar to brassinolide in stimulating the growth of

Arabidopsis thaliana roots, an action probably mediated by ethylene (Tsurumi et al., 2000). In an earlier study, the effects of steroidal saponin protodioscin were compared with those of brassinosteroid 24-epibrassinolide, indole-3-acetic acid (IAA), or abscisic acid (ABA) in the weed *B. pilosa* (Mito et al., 2019). It was demonstrated that protodioscin does not mimic the mode of action of individual phytohormones but it induces oxidative stress in primary roots, as suggested by the increased level of lipoperoxidation products and the activation of H_2O_2 scavenging enzymes. Moreover, a drastic change in root morphology of *B. pilosa* treated with protodioscin was also observed, an effect that has not been previously investigated in detail (Mito et al., 2019).

The morphogenic responses in seedlings have been observed in many stress conditions as a part of a strategy aiming to limit the plant stress exposure and to contribute to their tolerance of external toxicants (Potters et al., 2007). The detailed morpho-anatomy analysis through microscopic techniques has been demonstrated to be a valuable approach in the elucidation of the action mechanisms of many natural and synthetic compounds (Müller and Schmidt, 2004; Sánchez-Moreiras and Reigosa, 2018).

Although protodioscin may potentially contribute to the weed suppression effects of *U. ruziziensis* mulches in the field (Mito et al., 2019), weed species can exhibit different sensitivity to this saponin, as occur for synthetic herbicides. A factor influencing the sensitivity to synthetic herbicides is the distinct anatomy among the eudicot and monocot plant species (Kelley and Riechers, 2007; Sterling, 1997), which could define the selectivity of their actions (Carvalho et al., 2009). Therefore, a detailed investigation on the mode of action of protodioscin and extracts of *U. ruziziensis*, rich in this saponin, on different weeds could support the utilization of *U. ruziziensis* in the cropping/intercropping system as an alternative method for weed control in the field.

Thus, the present study aimed to compare the biochemical and morphological responses of a dicot *Ipomoea grandifolia* and a monocot *Digitaria insularis* weed to treatments with the protodioscin and the saponin-rich butanolic extract from the straw of *U. ruziziensis*. The two weeds are among the most troublesome weeds in the field due to the high prevalence of their biotypes being resistant to herbicides, particularly glyphosate (Carvalho et al., 2011; Pazuch et al., 2017). In these weeds, the anatomy and the morphology of the root systems were examined along with measurements of several biochemical parameters related to energy metabolism and antioxidant defense systems.

2. MATERIALS AND METHODS

2.1. Reagents

Protodioscin (Fig. 1), was purchased from Aktin Chemicals Inc. (The Republic of China) with 98% purity. Thiobarbituric acid (TBA), 2',7',-dichlorofluorescin diacetate (DCFDA), pyrogallol, nitroblue tetrazolium (NBT), ascorbic acid (AsA), glutathione (GSSG), enzymes and coenzymes were

purchased from the Sigma-Aldrich Company (St. Louis, USA). All the other solvents and reagents were of the best available grade.

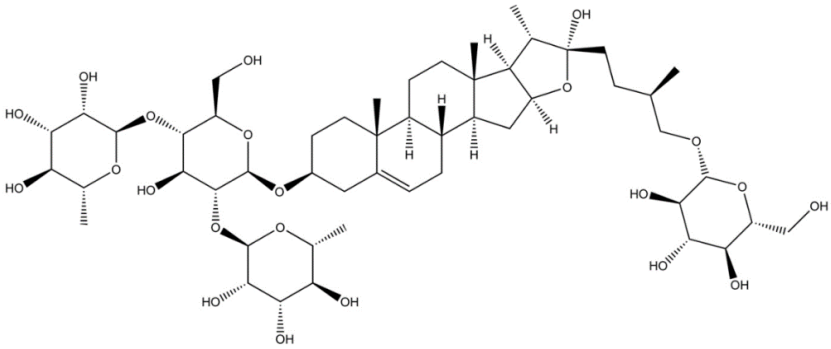

Figure 1 - Chemical structure of the saponin protodioscin.

2.2. Plant material

Urochloa ruziziensis (R. GERM. & C. M. EVRARD) CRINS was cultivated in an open field at the Experimental Farm of the University of Maringá, Iguatemi district, State of Paraná, Brazil (23° 20' 58.86" S and 52° 04' 27.56" W). The main physicochemical properties of the soil were pH of 6.9, 86% sand, 3% silt, 11% clay, and 6.08 g dm^{-3} of organic carbon. Plant aerial parts, collected in the pre-flowering stage (90 to 100 days after emergence), were dried in a drying oven with forced ventilation at room temperature, and then ground into small pieces with a ball mill. Plant material was initially extracted with cold hexane to remove superficial waxes. The residue was then extracted with 95% cold methanol by thorough maceration. After the solvent was removed under vacuum on a rotary evaporator at 33–35 °C, the crude methanolic extract was obtained. This extract was dissolved in about 1.0 L methanol/water (1/1, v/v) and subjected to sequential liquid-liquid chromatographic extractions using organic solvents with increasing polarity: hexane<dichloromethane<ethyl acetate< butanol. At each extraction stage, the resulting residues were extracted 3 times using a separatory funnel with 150 mL of each solvent. The residues obtained after solvent evaporation in a rotary evaporator adjusted to a temperature adequate for each solvent resulted in hexane (Hex. F.), dichloromethane (D. F.), ethyl acetate (E. A. F.), and butanolic (But. F.) fractions. In this study, the saponin-rich butanolic fraction was used. Seeds of *Digitaria insularis* (L.) MEZ ex EKMAN and *Ipomoea grandifolia* (DAMMER) O'DONELL were purchased from Cosmos Agrícola Produtos e Serviços Rurais LTDA-Brazil.

2.3. Seed germination and seedling initial growth

Seeds of *I. grandifolia* and *D. insularis* had been previously selected for size and appearance. The seeds of *I. grandifolia* were scarified with sulfuric acid for 45 min to break seed dormancy. After washing with distilled water, seeds were placed in plastic boxes (Gerbox® 110 × 110 × 50 mm) containing 40 mL of semi-solid agar 0.8% (w/v) with protodioscin at 50, 100, and 250 μg mL^{-1}

concentrations and the But. F. of *U. ruziziensis* (Bf*Ur*) at 100, 250, and 500 µg mL^{-1}. Protodioscin and the Bf*Ur* were dissolved in the agar medium before its solidification. Each treatment, including controls, was replicated five times, and each replicate consisted of 50 seeds. Boxes were randomly placed in a germination chamber (photon flux density of approximately 230 $\mu mol.m^{-2}.s^{-1}$). The *I. grandifolia* was maintained at a constant temperature of 30 °C, with a 12-h photoperiod (light/dark) and *D. insularis* was maintained in photoperiod to 8/16 h (light/dark) at 30 °C and 20 °C, respectively. At the end of treatment (120 hours), roots and aerial parts of seedlings were excised for measurements of their lengths and fresh weights. Then, plant materials were placed into the oven for 48 h at 60 °C, to determine their dry weight. The dose-response curves of primary root length were used to estimate the concentrations of protodioscin and the Bf*Ur*, which caused 50% inhibition of root growth (IC_{50} values) in *I. grandifolia* and *D. insularis.*

The germinated seeds were counted daily until 120 h of treatment for calculations of mean germination time ($\bar{t}$), speed of germination (S), and speed of accumulated germination (S_A) (Chiapusio et al., 1997; Labouriau and Osborn, 1984). The mean germination time was calculated by equation 1:

$$\bar{t} = \sum n_i t_i \Big/ \sum n_i \qquad (1)$$

where $\bar{t}$ is the mean germination time, and n_i is the number of germinated seeds between the times t_{i-1} and t_i. The speed of germination was calculated by equation 2:

$$S = (N_1/T_1) + (N_2 - N_1) \times 1/2 + (N_3 - N_2) \times 1/3 + \ldots (N_n - N_{n-1}) \times 1/n \qquad (2)$$

where S represents the speed of germination and N represents the proportion of germinated seeds obtained in the first (T_1), second (T_2), third (T_3), … , ($n - 1$) hours. The speed of accumulated germination was calculated by equation 3:

$$S_A = (N_1/T_1) + (N_2/T_2) + (N_3/T_3) + \ldots (N_n/T_n) \qquad (3)$$

where S_A represents the speed of accumulated germination and N represents the proportion of germinated seeds at time (T_1), time (T_2), time (T_3), $\cdots$(T_n), hours.

2.4. Respiratory activity measurements in primary root apexes

The respiratory activity of the root apexes of both species, treated with or without Bf*Ur* or protodioscin for 120 h at their respective IC_{50} concentrations, was measured at 25 °C using a Clark type electrode that was inserted into an acrylic chamber and connected to a polarograph (Ishii-Iwamoto et al., 2006). Approximately 20 mg of the root apexes were cut into segments with lengths of 2–4 mm, and they were immediately placed into the oxygen electrode vessel containing 2 mL of a

nutrient solution (pH 5.8) containing 2 mM $Ca(NO_3)_2$, 2 mM KNO_3, 27 μM $FeCl_3$, 0.43 mM NH_4Cl, 0.75 mM $MgSO_4$ and 20 μM NaH_2PO_4. The rate of oxygen consumption was expressed in nanomoles of oxygen consumed per minute per amount of tissue (milligrams), assuming the initial concentration of dissolved oxygen of 240 μM at 25 °C. To estimate the contribution of mitochondrial ferrocytochrome-*c*:oxygenoxidoreductase (COX; EC 1.9.3.1) to the overall O_2 uptake, 200 μM KCN was added to the reaction medium approximately 5 minutes after the addition of the apexes (KCN-sensitive-respiration). The residual oxygen consumption was defined as KCN-insensitive respiration.

2.5. Measurements of antioxidant enzyme activities

Approximately 25–100 mg of roots, treated or not with the Bf*Ur* or protodioscin for 120 h at the respective IC_{50} concentrations, were transferred to a cold mortar and macerated with 1 mL of a medium containing 0.1 M phosphate buffer (pH 6.8) and 0.1% polyvinylpyrrolidone (PVP). The extracts were then centrifuged at 4 °C, for 30 min, at 7,400 × *g*. The supernatant was used as the source of the enzymes. All the operations were carried out at 4 °C.

Catalase (CAT; EC 1.11.1.6) activity was measured in a medium containing 50 mM phosphate buffer (pH 6.8), 5.8 mM H_2O_2, and the enzyme extract (0.01–0.05 mg protein). The H_2O_2 consumption was measured by a spectrophotometer at 240 nm (ε = 43.6 M^{-1} cm^{-1}) (Aebi, 1984).

Peroxidase activity (POD; EC 1.11.1.7) was measured in a medium containing 50 mM phosphate buffer (pH 6.8), 6 mM H_2O_2, 0.15 mM pyrogallol, and the enzyme extract (0.01–0.05 mg of protein). The POD activity was calculated by determining the amount of purpurogalin formed by a spectrophotometer at 420 nm (ε = 2.64 mM^{-1} cm^{-1}) (Pütter, 1974).

Glutathione reductase (GR; EC 1.8.1.7) activity was measured in a medium containing 50 mM phosphate buffer (pH 7.5), 1 mM GSSG, 0.1 mM NADPH, and the enzyme extract (0.01–0.05 mg of protein). The NADPH consumption was measured by a spectrophotometer, at 340 nm (ε = 6.22 mM^{-1} cm^{-1}) (Foyer and Halliwell, 1976).

Superoxide dismutase activity (SOD; EC 1.15.1.1) was monitored according to Giannopolitis and Ries (1977). The reaction medium contained 50 mM phosphate buffer (pH 6.8), 13 mM methionine, 70 μM tetrazolium nitroblue oxidation (NBT), 2 μM riboflavin, and the enzyme extract (0.025–0.075 mg of protein). The reaction started with exposure to light (approximately 230 $\mu mol.m^{-2}.s^{-1}$) in which it was maintained for 60 minutes at 30 °C. A unit of SOD (U) activity was defined as the amount of enzyme needed to inhibit the NBT oxidation by 50%. The photoreduction rate was measured by a spectrophotometer at 560 nm and expressed as U mg^{-1} of SOD to protein.

The activity of ascorbate peroxidase (APX; EC 1.11.1.11) was measured in a medium containing 50 mM phosphate buffer (pH 6.8), 0.5 mM ascorbate, 15 mM H_2O_2, and the enzyme extract (0.01–0.05 mg protein). The ascorbate oxidation was measured by spectrophotometer at 290 nm (ε = 2.8 mM^{-1} cm^{-1}) (Nakano and Asada, 1981).

2.6. Determination of the Reactive Oxygen Species (ROS) content

The determination of ROS was carried out according to the procedure of Jambunathan (2010), with some modifications. Approximately 25–100 mg of *D. insularis* and *I. grandifolia* roots treated or not with the Bf*Ur* or protodioscin (IC_{50}) were pulverized with liquid nitrogen using a mortar and pestle. Then, the material was transferred to a plastic tube, mixed with 2 mL of 10 mM Tris-HCl buffer (pH 7.2), and centrifuged at 12,000 × *g* for 20 minutes and 4 °C. The supernatants were transferred to glass, diluted 1:20 with Tris-HCl buffer. To start the fluorescence reaction with ROS, 10 µL of 2',7',-dichlorofluorescin diacetate (DCFDA) (1 mM prepared in dimethyl sulfoxide DMSO) was pipetted into each tube that was rapidly homogenized with a vortex and kept in the dark for approximately 10 min. The wavelengths (λ) used were 504 nm and 526 nm for excitation and emission, respectively. The ROS contents were expressed in fluorescence units per microgram of fresh weight.

2.7. Determination of the malondialdehyde (MDA) and conjugated dienes content

Approximately 25–100 mg of roots, treated or not with the Bf*Ur* or protodioscin at the respective IC_{50} concentrations, were withdrawn and macerated with 0.5 mL of 96% ethanol at 4 °C. An aliquot of 0.2 mL of this homogenate was mixed with 0.8 mL of 2-thiobarbituric acid (TBA), dissolved in 10% trichloroacetic acid (TCA) in Falcon-type tubes. After incubation at 95 °C for 30 min, the reaction was stopped by placing the tube in an ice bath. The sample was centrifuged at 15,000 × *g* for 20 min. The absorbance of supernatant was measured at 532 nm and 600 nm. The difference between these two wavelengths was used to calculate the MDA content (ε = 155 mM^{-1} cm^{-1}) (Heath and Packer, 1968). The results were expressed as µmol g^{-1} (fresh weight).

To measure the conjugated dienes, a 75 µL aliquot of the homogenate was mixed in 1425 µL of 96% ethanol in an Eppendorf type tube, and then centrifuged at 20,000 × *g* for 20 min (Boveris et al., 1980). The absorbance of the supernatant was recorded by a spectrophotometer at 234 nm and 500 nm. The difference between these two wavelengths was used to calculate the conjugated dienes concentration, using $\varepsilon = 2.65 \times 10^4$ M^{-1} cm^{-1}. The results were expressed as µmol g^{-1} (fresh weight).

2.8. Determination of root permeability to ions

Roots treated or not with the Bf*Ur* or protodioscin, at the respective concentrations of IC_{50} were weighed and immersed in beakers containing 30 mL of deionized water for *I. grandifolia* and 20 mL for *D. insularis*, at room temperature. The roots were kept at rest for 4 h (T4), and the electrical conductivity was therefore measured with a conductivity meter (Tecnal TEC-4MP). Roots were then transferred to another beaker containing 30 mL or 20 mL of deionized water, according to the species,

boiled for 15 minutes and the electrical conductivity was again determined at room temperature (TF). The conductivity rate was determined by (T4 / TF + T4) x 100 and expressed as a percentage. The cell conductivity used for this experiment was number 1, and the standard cell was 146.9 μS cm^{-1}.

2.9. Analysis of the anatomy and morphology of seedling roots

Seedlings of *D. insularis* and *I. grandifolia* were grown for 120 hours in 0.8% agar medium, with or without the Bf*Ur* or protodioscin, at their respective IC_{50} concentrations, were randomly selected and then photographed using a Leica EZ4D stereomicroscope with a built-in digital camera.

For the anatomical analysis, the primary roots of *D. insularis* and *I. grandifolia* were fixed in Nawaschin CRAF fixative and stored in 70% ethanol. Treated and untreated root samples, already fixed in CRAF, were randomly selected and embedded in Leica historesin, according to the manufacturer's instructions. The historesin-included materials were sectioned in a rotation microtome to produce cross-sections (7 μm thick), used in the assembly of permanent histology glass slides. The sections were made at the base of *D. insularis* roots and in the middle region of *I. grandifolia* roots. Sections were stained with toluidine blue in acetate buffer (pH 4.7) (O'Brien et al., 1964). The photographic documentation of the slides was performed with a Leica ICC 50 light microscope with a digital camera coupled using the Leica Application Suite software version 1.8.

2.10. Determination of proteins

The protein content of the primary root extracts was determined according to Bradford (1976), using bovine serum albumin as standard. The range of concentrations in the standard curve was 0.5 to 20 mg% with an r^2 of 0.934. Each plant extract was diluted to reach a protein concentration of less than 15 mg%.

2.11. Statistical analysis

The data presented in the graphs were expressed as mean ± standard errors (S.E.) of independent preparations; these were analyzed by analysis of variance (ANOVA), with significant differences between the means identified by Tukey's Honestly Significant Difference (HSD) test ($p \leq 0.05$) using RStudio software. The IC_{50} concentrations were calculated by numerical interpolation using the cubic spline function of GraphPad Prism 5 software.

3. RESULTS

3.1. Effects of the Bf*Ur* and protodioscin on the germination and initial growth of *D. insularis* and *I. grandifolia*

Both the Bf*Ur* and protodioscin induced differential effects on the germination of *D. insularis* and *I. grandifolia* at the concentrations tested (Table 1). The germination indices of *I. grandifolia* were not significantly modified, but in *D. insularis*, the Bf*Ur* caused a dose-dependent inhibition in the percentage of germination (G%), the speed of germination (*S*), and the speed of accumulated germination (S_A), while protodioscin affected the indices at the highest concentration (250 µg mL^{-1}). The comparison of the Bf*Ur vs* protodioscin in *D. insularis* at 250 µg mL^{-1} displayed a reduction of the maximal percentage of germination (%), the speed of germination (*S*), and the speed of accumulated germination (S_A) by 29%, 40%, and 29% of the extract, respectively, compared to 45%, 50% and 57% of protodioscin. Both treatments increased the mean time of germination ($\bar{t}$) by nearly 20% at 250 µg mL^{-1} (Table 1).

Table 1– Germination percentage (G%), speed of germination ($S^{¥}$), speed of accumulated germination ($S_A^{¥}$), and mean germination time ($\bar{t}$) of *D. insularis* and *I. grandifolia* grown for 24–120 hours, treated with 0 (control), 100, 250, and 500 µg mL^{-1} of Bf*Ur* or 50, 100, and 250 µg mL^{-1} of protodioscin.

Weed species	Treatment (µg mL^{-1})		(G%)	($S^{¥}$)	($S_A^{¥}$)	($\bar{t}$)(h)
D. insularis	Bf*Ur*	0	68.4±4.91a	0.20±0.02a	1.39±0.10a	65.5±2.12a
		100	52.4±4.58ab	0.13±0.02b	1.07±0.12ab	64.5±1.53a
		250	48.8±0.80b	0.12±0.00bc	0.98±0.03b	66.1±1.27a
		500	39.2±3.32b	0.08±0.01c	0.60±0.05c	79.0±1.28b
	Protodioscin	0	65.6±7.25a	0.18±0.02a	1.47±0.15a	60.8±0.52a
		50	55.2±4.59a	0.15±0.01a	1.16±0.09a	63.9±1.52ab
		100	65.2±3.14a	0.17±0.01a	1.26±0.10a	68.3±1.87ab
		250	36.0±2.45b	0.09±0.01b	0.63±0.04b	74.2±4.50b
I. grandifolia	Bf*Ur*	0	80.40±1.47a	0.78±0.01a	3.64±0.03a	29.01±0.72a
		100	75.2±1.86a	0.76±0.02a	3.50±0.07a	26.5±0.77a
		250	82.0±1.41a	0.86±0.02b	3.99±0.07b	26.9±0.86a
		500	79.2±2.33a	0.80±0.03ab	3.70±0.12ab	27.6±0.10a
	Protodioscin	0	81.2±1.62a	0.73±0.01a	3.47±0.06a	31.1±0.83a
		50	75.2±3.01a	0.66±0.02a	3.18±0.11a	32.2±0.99a
		100	82.0±3.69a	0.73±0.03a	3.53±0.15a	30.9±0.89a
		250	75.2±4.03a	0.68±0.03a	3.23±0.15a	30.7±1.03a

¥Seeds germinated per hour**.** Values are means ± SE (n=5). Different letters indicate means that differ significantly, according to Tukey's HSD test at $p \leq 0.05$

Despite the lack of effect on the germination of *I. grandifolia*, the initial development of its seedlings was inhibited by both the Bf*Ur* and protodioscin treatments, as was also occurring in *D. insularis.* In both weeds, the growth of roots and the aerial parts were altered (Fig. 2), with a more pronounced reduction in the length of primary roots. In general, *I. grandifolia* was less sensitive than *D. insularis* and the Bf*Ur* was less active than protodioscin, as revealed by the IC_{50} values for the root length reduction. In *I. grandifolia,* the IC_{50} values were 230 μg mL^{-1} for Bf*Ur* and 54 μg mL^{-1} for protodioscin. The corresponding values were 108 μg mL^{-1} and 34 μg mL^{-1} in *D. insularis.* The growth of aerial parts of *I. grandifolia* was more extensively reduced by the Bf*Ur* treatment when compared with *D. insularis,* and, therefore, the fresh weight of seedlings was reduced only in *I. grandifolia.* Protodioscin was more active than the Bf*Ur* treatments in causing a dose-dependent inhibition in the length of aerial parts and the fresh weights of seedlings in both *I. grandifolia* and *D. insularis*. The comparison of the Bf*Ur vs* protodioscin in *I. grandifolia* at 250 μg mL^{-1} displayed a reduction of the aerial part lengths, fresh weights, and dry weights of seedlings by 23.5%, 33.9%, and 0% by Bf*Ur*, respectively, compared to 50.3%, 43.3%, and 19.8% by protodioscin. In *D. insularis,* protodioscin at 250 μg mL^{-1} significantly altered the length of the aerial parts (–46%) and the fresh weight of seedlings (–31.8%) without significant change by the Bf*Ur* when compared with their respective controls (Fig. 2e, g). The subsequent biochemical and morpho-anatomical studies were performed with roots of seedlings treated with the IC_{50} values of Bf*Ur* and protodioscin for the root length reduction in the two assayed weeds.

3.2. Effects of the Bf*Ur* and protodioscin on the respiratory activity of root apexes of *D. insularis* and *I. grandifolia*

To investigate whether the inhibition of the primary root growth caused by the Bf*Ur* and protodioscin in both weed species was related to an interference with the energy metabolism, the respiratory activity of the root apexes exposed to their respective IC_{50} concentration was assayed.

The respiratory activity of the control seedlings revealed a significant difference between the weeds *D. insularis* and *I. grandifolia.* The total O_2 consumption (total respiration) of the root apexes of *D. insularis* was remarkably higher compared to those of *I. grandifolia* (Fig. 3). The fraction of total respiration inhibited by the addition of KCN (KCN-sensitive respiration) represents the mitochondrial cytochrome oxidase (COX) respiration that is coupled to ADP phosphorylation, while the remainder of total respiration (KCN-insensitive respiration) is due to the oxygen consumption by other mitochondrial oxidases, such as alternative oxidase (AOX; EC 1.10.3.11) and extra-mitochondrial oxidases (Ishii-Iwamoto et al., 2006). This discrimination revealed that most of the respiration of *D. insularis* roots was due to KCN-insensitive respiration, which represented 53% of total respiration, while the corresponding value was 28% in *I. grandifolia* roots (Fig. 3).

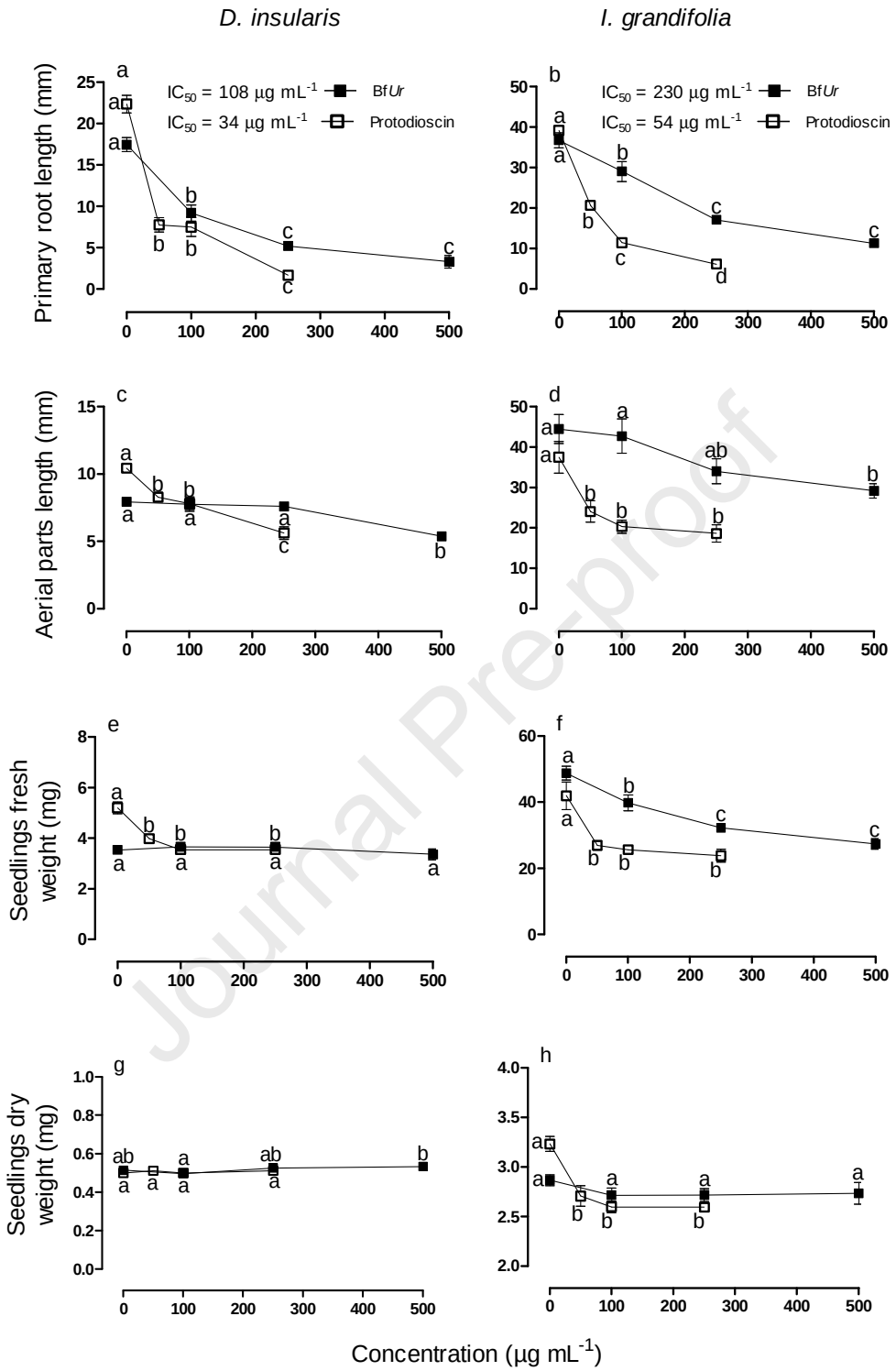

Figure 2 - Effects of But. F. of *U. ruziziensis* (Bf*Ur*) and protodioscin on root lengths (a, b), aerial part lengths (c, d), fresh weights (e, f), and dry weights (g, h) of the seedlings of *D. insularis* and *I. grandifolia*, respectively, treated for 120 hours. The concentrations tested were the respective IC_{50} of each species. Values are means ± SE (n=5). Different letters indicate that means differed significantly according to Tukey's HSD test at $p \leq 0.05$

The rate of KCN-insensitive respiration was 6.2-fold higher in *D. insularis* compared to *I. grandifolia* and the corresponding value for KCN-sensitive respiration was 2.1-fold.

The responses of *D. insularis* and *I. grandifolia* to the Bf*Ur* or protodioscin treatments at their respective IC_{50} values were markedly different. The respiratory activities of *D. insularis* were not significantly affected by Bf*Ur* or protodioscin (Fig. 3c). In contrast, in *I. grandifolia*, the Bf*Ur* induced a 92% increase in total respiration, which was due to an increase in the KCN-sensitive (+101%) respiration compared to the respective control values (Fig. 3b, d, f). Protodioscin was inactive (Fig. 3f).

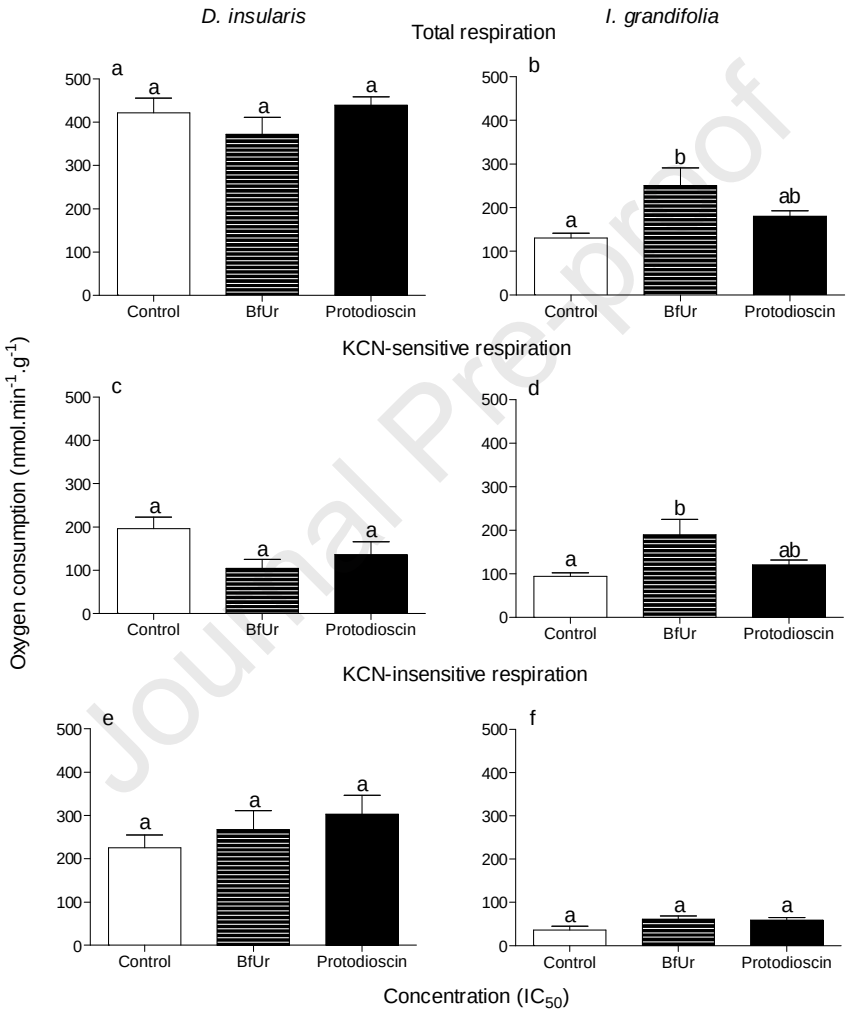

Figure 3 – Effects of But. F. of *U. ruziziensis* (Bf*Ur*) and protodioscin on the respiratory activity of root apexes from the primary roots of *D. insularis* and *I. grandifolia* treated for 120 hours. The concentrations tested were the respective IC_{50} values of each species. The oxygen consumption of the root apexes was measured in the absence or presence of the KCN inhibitor: total respiration (a, b), KCN-sensitive respiration (c, d), and KCN-insensitive respiration (e, f). Each data point is the mean ± SE (n=6,7). Different letters indicate means that differ significantly, according to Tukey's HSD test at $p \leq 0.05$

3.3. Effects of the Bf*Ur* and protodioscin on the ROS, malondialdehyde (MDA), and conjugated dienes content and on the ions permeability in the roots of *D. insularis* and *I. grandifolia*

An increase in oxygen consumption due to the extra-mitochondrial oxidases or alternative oxidase (KCN-insensitive respiration) are generally associated with an increased ROS generation, which in turn can generate a cellular oxidative stress (Vanlerberghe, 2013). These hypotheses were investigated by evaluating the ROS content and some products resulting from the ROS attack on membrane polyunsaturated fatty acids, including MDA (Kappus, 1985) and conjugated dienes (Recknagel and Glende, 1984).

In untreated seedlings, the content of ROS, MDA, and conjugated dienes was significantly higher in roots of *D. insularis* than in *I. grandifolia* (Fig. 4). In general, the Bf*Ur* or protodioscin induced an increase in the ROS content in both weed species (Fig. 4a, b), although the relative increment was more marked in *I. grandifolia* than in *D. insularis.* In *I. grandifolia*, the ROS content increased by 182% (Bf*Ur*) and 139% (protodioscin) compared to the untreated seedlings. In *D. insularis*, only protodioscin treatment increased the ROS content (+86%).

In *D. insularis*, the MDA content remained unaltered in both treatments, although an increase of 46% in the content of the conjugated diene was found in the Bf*Ur* treatment. In *I. grandifolia*, a decrease in the MDA content was found in both the Bf*Ur* treatment (–41%) and protodioscin (–31%). A contrasting effect was found in the content of conjugated dienes; Bf*Ur* and protodioscin induced an increase of 106% and 104%, respectively, when compared with their controls.

The possibility of functional damage in root cells was analyzed by ion permeability measurements (Fig. 4g, h). The Bf*Ur* treatment induced a similar increase in the ion permeability in *D. insularis* (+57%), and *I. grandifolia* (+53%); protodioscin was active in *I. grandifolia* (+52%) but not in *D. insularis.*

3.4. Effects of the Bf*Ur* and protodioscin on the activity of the antioxidant enzymes in the roots of *D. insularis* and *I. grandifolia*

The changes in ROS, MDA, and conjugated dienes could be related to the capacity of the antioxidant defense system in the two assayed weeds. The comparison of the enzymatic activities in the control seedlings, based on the protein content in the root extract, indicated that the activities of SOD, POD, CAT, and APX activities are higher in *D. insularis* than in *I. grandifolia*, while GR activity is similar in both species (Fig. 5). The Bf*Ur* and protodioscin (IC_{50}) treatments exerted different effects on the two species. In *D. insularis*, none of the assayed enzymes were modified by the Bf*Ur* and protodioscin treatments compared to the respective controls (Fig. 5a, g, i). An exception was a reduction of 34% in the activity of POD by the Bf*Ur* treatment. In *I. grandifolia*, when comparing the effects of both treatments on each enzyme, similar effects were found.

The SOD activity was increased by 111% and 117% by the Bf*Ur* and protodioscin, respectively, the CAT activity was reduced by 49% and 32%, respectively, and the APX and GR activities were not modified when compared with their respective controls. The POD activity was stimulated only by the protodioscin treatment (+33%).

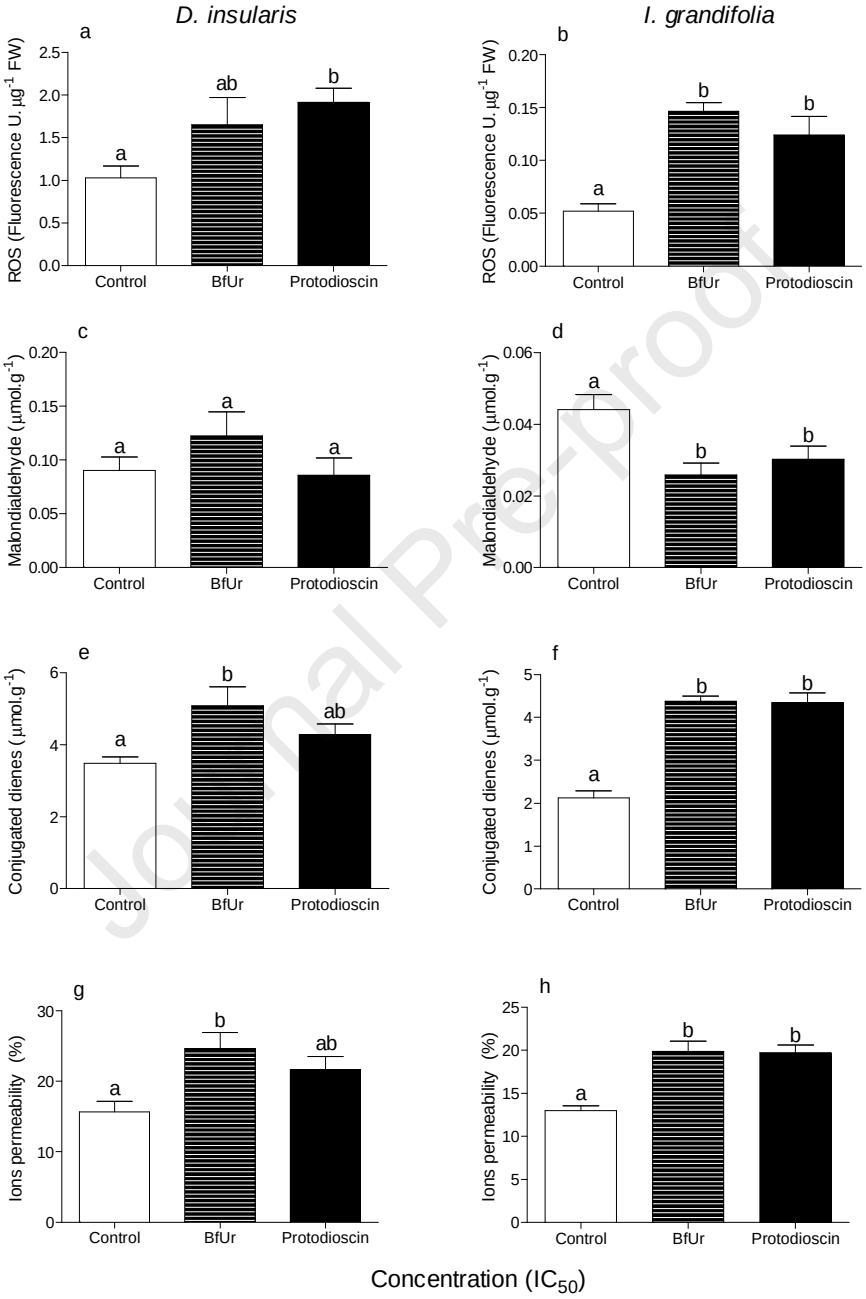

Figure 4 – Effects of the But. F. of *U. ruziziensis* (Bf*Ur*) and protodioscin on the ROS content (a, b), malondialdehyde (c, d), conjugated dienes (e, f), and ion permeability (g, h) of the *D. insularis* and *I. grandifolia* roots incubated for 120 hours. The tested concentrations were the respective IC_{50} values of each species. Each data point is the mean ± SE (n=4–6). Different letters indicate means that differ significantly, according to Tukey's HSD test at $p \leq 0.05$

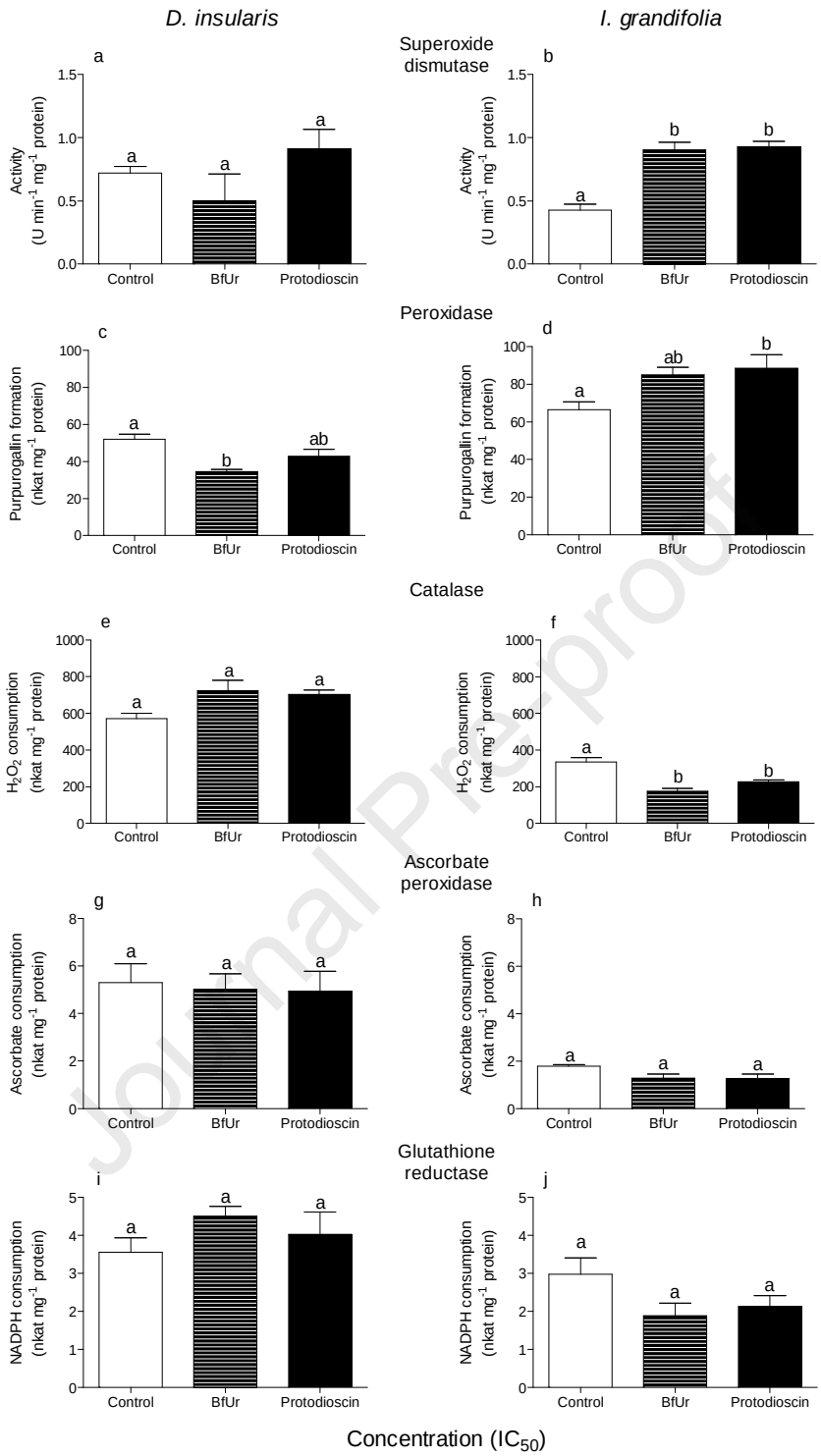

Figure 5 – Effects of But. F. of *U. ruziziensis* (Bf*Ur*) and protodioscin on the enzymes of the antioxidant defense system from roots of *D. insularis* and *I. grandifolia* treated for 120 hours. The concentrations tested were the respective IC_{50} values of each species. Enzymes: superoxide dismutase (a, b), peroxidase (c, d), catalase (e, f), ascorbate peroxidase (g, h), and glutathione reductase (i, j). Each data point is the mean ± SE (n=5,6). Different letters indicate means that differ significantly, according to Tukey's HSD test at $p \leq 0.05$

3.5. Effects of the Bf*Ur* and protodioscin on the morphology and anatomy of *D. insularis* and *I. grandifolia* roots

As can be seen in Figs. 6 and 7, the *D. insularis* and *I. grandifolia* seedlings treated with the Bf*Ur* and protodioscin exhibited a noticeable shortening in the length of their primary roots when compared to the respective controls, thus reflecting the values obtained in the biometric measurements (Fig. 2a, b). The roots also showed a change in density of the root hairs which were abundant in both the *D. insularis* (Fig. 6a, c) and *I. grandifolia* (Fig. 7a) control roots, and became minimal in the treatments (Figs. 6d, f, 7d, g). This feature was highlighted in the Figs. 1Sa, b, c and Figs. 2Sa, b, c in Supplementary Material. In addition, the browning of the roots caused by the treatments in both weed species is also noteworthy (Figs. 6e, g, 7e, h).

Despite these similarities, a distinct morphological change in the root architecture was observed in the weeds. In the control roots of *I. grandifolia* the lateral roots appeared between the base and the middle region of the primary roots (Fig. 7a, b, c) and in seedlings treated with the Bf*Ur* and protodioscin, many lateral roots appeared in the entire extent of the primary root, including near the apex were observed (Fig. 7e, f, h, i). These roots were shorter and displayed more browning than those the control displayed. On the other hand, in *D. insularis* the number of adventitious roots was not increased by the treatments, but on the contrary, a reduction was apparent (Fig. 6a, d, f).

Fig. 8 shows the images of cross-sections of *D. insularis* roots. The control roots consisted of a uniseriate epidermis, with thin-walled and unicellular hairs (Fig. 8a, c), parenchymatous cortex with three cell layers, in which the exodermis is indistinct and the endodermis has U-thickened cells (Fig. 8a), a vascular cylinder composed of a uniseriate parenchyma pericycle, interrupted by protoxylem cells, and five xylem strands alternated with phloem strands. Therefore, the roots are pentarchal with a central metaxylem element (Fig. 8b).

The treatment with the Bf*Ur* and protodioscin did not induce substantial changes in the cell organization in the primary roots (Fig. 8d, g), but changed the morphology of cells. In the roots of seedlings exposed to Bf*Ur*, the epidermis was discontinuous, with more rounded cells, while the exodermis presented cells with U-shaped parietal thickening (Fig. 8f). The endodermal cells were compressed and had a reduced lumen (Fig. 8e). The primary xylem appears in the central cylinder with tracheal elements and fibers, both with lignified and thicker cell walls (Fig. 8e). In the presence of protodioscin, the subepidermal layer (exodermis) exhibited cells with thickening in U shape, similar to the endodermis cells (Fig. 8g, i). The primary xylem also has tracheal elements, but no fibers, and parenchymatic cells less stained (Fig. 8h).

As a dicot species, the anatomy of the *I. grandifolia* primary roots presented a distinct organization with respect to *D. insularis*. The control roots consisted of the uniseriate epidermis, with cells of isodiametric contour (Fig. 9a, c). In the cortex (Fig. 9a), the endodermis with Casparian strip and pluriseriate parenchyma were distinguished, where large cells of secretory aspect, which undergo

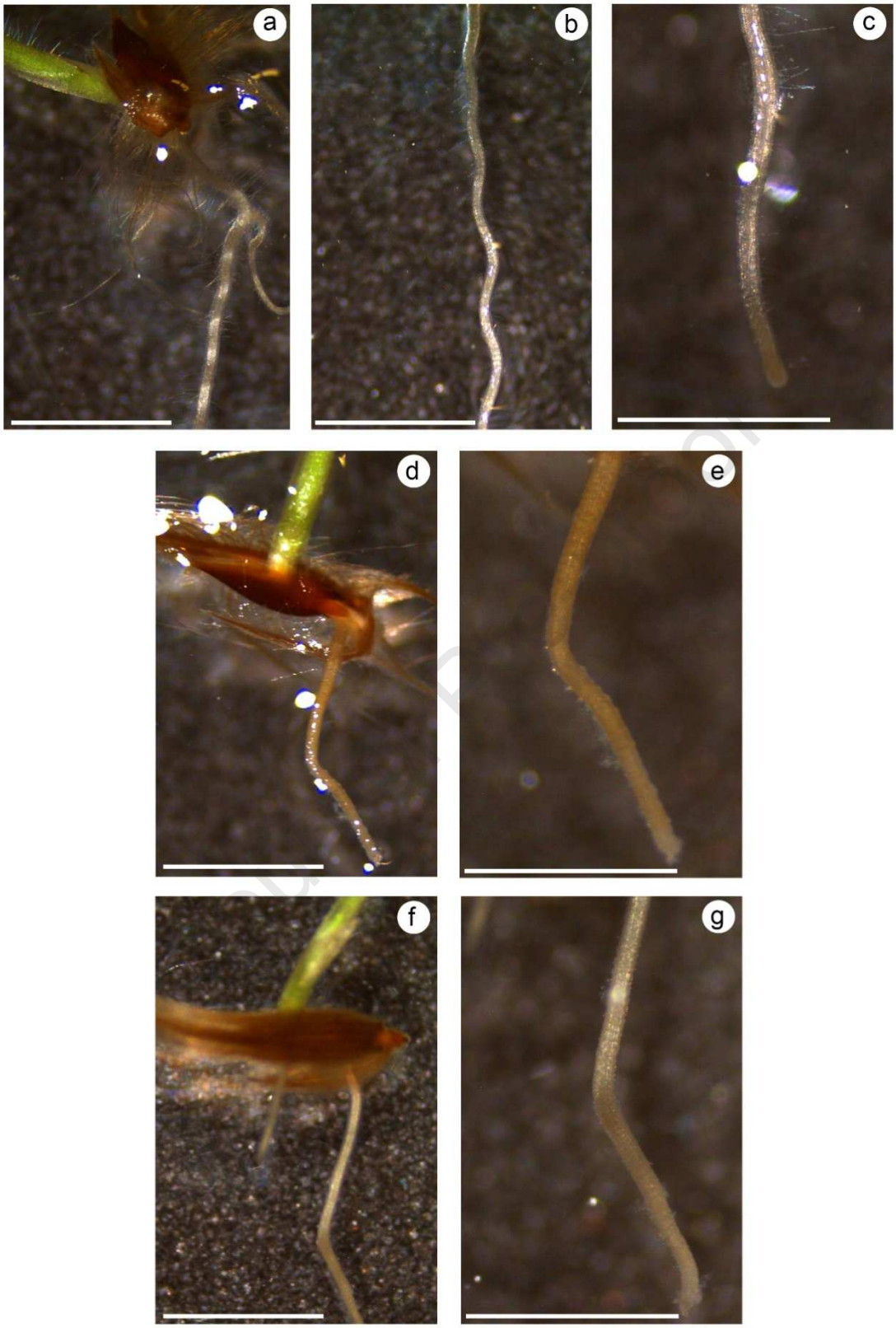

Figure 6 – Root morphology of *D. insularis* treated for 120 hours. The concentrations of Bf*Ur* and protodioscin were the IC_{50} values 108 and 34 µg mL^{-1}, respectively. Control (a-c); Bf*Ur* (d-e), protodioscin (f-g). Scale: (a, b, d, f)—3 mm and (c, e, g)—2 mm.

Figure 7 – Root morphology of *I. grandifolia* treated for 120 hours. The concentrations of Bf*Ur* and protodioscin were the IC_{50} values 230 and 54 µg mL^{-1}, respectively. Control (a–c); Bf*Ur* (d–f), protodioscin (g–i). Scale: (a, b, d, e, g, h)—3 mm and (c, f, i)—2 mm.

dissolution of the cell wall, formed remarkable cavities in the cortex (Fig. 9a, b, c). In the vascular cylinder, the pericycle was parenchymatic and uniseriate, with light and radially elongated cells (Fig. 9b). The cylinder was still tetrarchal, with four phloem strands alternated with those of xylem (Fig. 9b).The treatments with the Bf*Ur* exhibited similar changes to those observed in the protodioscin treatment compared to the controls. The epidermis exhibits an apparent thickening of the cell wall (Fig. 9f, i). In the cortex, the endodermis did not differ from that of the control roots, but the parenchyma also had cavities, which were higher in number in the Bf*Ur* treatment and lower in number in the protodioscin treatment when compared to their respective control seedlings (Fig. 9a, d, g). The Bf*Ur* induced the formation of the vascular cambium with procambial origin in the vascular cylinder, which was not evident in the control roots (Fig. 9b, e). The root was also tetrarchal, with enlargement of vascular tissues, and as can be observed, a wide crimped tube occurs in each phloem strand (Fig. 9e).

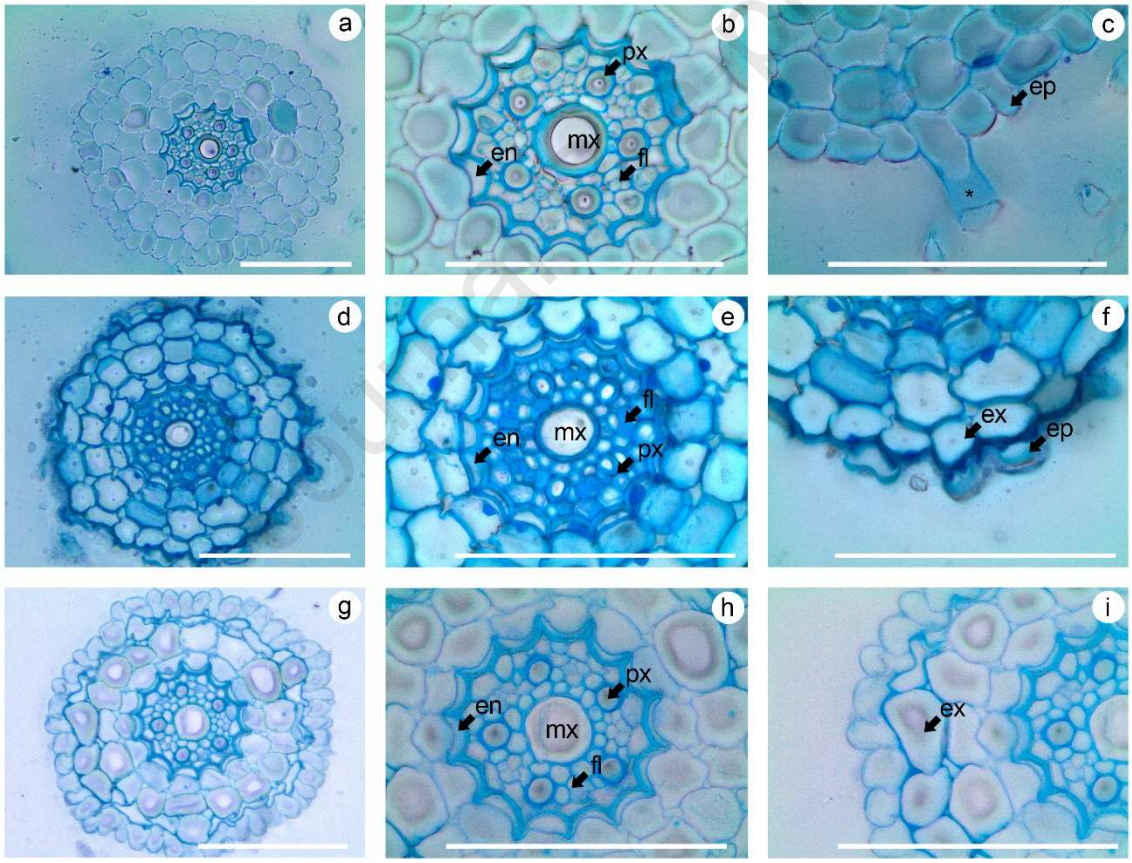

Figure 8 – Anatomical details of the roots of *D. insularis* treated for 120 hours. The IC_{50} concentrations of But. F. of *U. ruziziensis* (Bf*Ur*) and protodioscin were 108 and 34 µg mL^{-1}, respectively. Control (a–c); Bf*Ur* (d–f), protodioscin (g–i). Overview of the root, showing the organization of the root tissues (a, d, g), view of the central cylinders (b, e, h) and view of the cortex and epidermis (c, f, i), (ep: epidermis; *: root hair; en: endodermis; ex: exodermis; fl: primary phloem; mx: metaxylem; px: protoxylem). Scales: (a, b, c, d, e, f, g, h, i)—0.1mm.

Finally, in the protodioscin-treated roots, some anatomical differences were observed (Fig. 9a, g). The epidermis was discontinuous, formed by tangentially elongated cells (Fig. 9i). In the cortex, the endodermis was present, as well as parenchymal tissue (Fig. 9h). The cortical cavities were enlarged through the fusion of the gaps, compressing the cortex (Fig. 9g). The root cylinder had a uniseriate parenchyma pericycle and was tetrarchal (Fig. 9h), but a significant increase of the vascular tissues was also evident, where it was possible to observe the development of the vascular cambium of procambial origin (Fig. 9h), as also found in the Bf*Ur* treatment (Fig. 9e).

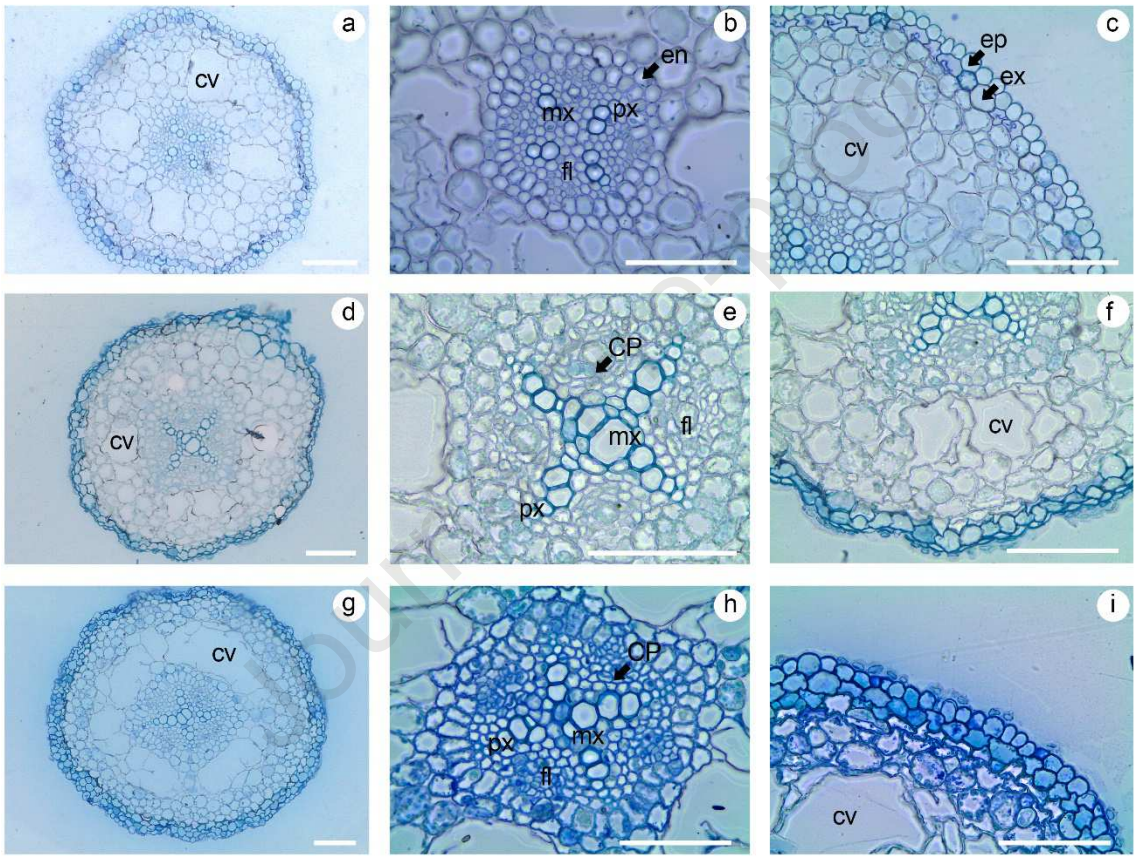

Figure 9 – Anatomical details of *I. grandifolia* roots treated for 120 hours. The concentrations of But. F. of *U. ruziziensis* (Bf*Ur*) and protodioscin were the IC_{50} values 230 and 54 µg mL^{-1}, respectively. Control (a–c); Bf*Ur* (d–f), protodioscin (g–i). Overview of the root, showing the organization of the root tissues (a, d, g), view of the central cylinders (b, e, h) and view of the cortex and epidermis (c, f, i), (ep; epidermis; en: endodermis; ex: exodermis; fl: phloem; mx: metaxylem; px: protoxylem; CV: cavity; CP: vascular cambium with procambial origin). Scale: (a, b, c, d, e, f, g, h, i)—0.1 mm.

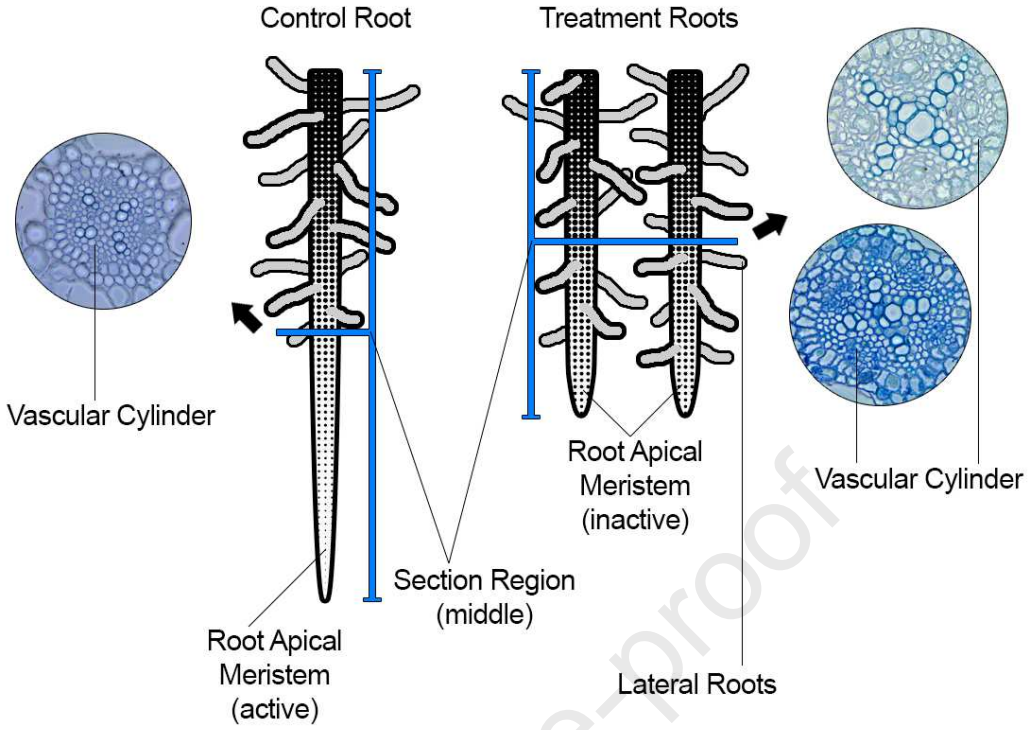

Figure 10 – Representation of the roots of *I. grandifolia* submitted to the anatomical analyzes, highlighting the differences in the degree of development of the vascular cylinder in control and treated roots. The blue lines represent the positions in roots, where the sections took place (middle region of each root) to perform the anatomical analyses. The gradient between black and white colors in the roots represents the degree of differentiation and development of the root tissues, where black represents a high differentiation, and white represents a low differentiation.

4. DISCUSSION

This study highlighted the different responses of the eudicot *I. grandifolia* and the monocot *D. insularis* weeds to the Bf*Ur* and the steroidal saponin protodioscin treatment. One of the remarkable species-specific differences was underlined by germination indices. The germination of *I. grandifolia* was weakly altered compared to *D. insularis*, which was strongly inhibited especially by the Bf*Ur*. Many factors may have contributed to this difference, including the structure and properties of the external seed coat, which can influence the uptake rate of the active substances during the seed imbibition process (Mitchell et al., 2017). Seeds of *D. insularis* are considerably smaller than those of *I. grandifolia*, a feature that could favor the diffusion of compounds into the developing embryo.

In addition, the Bf*Ur* at a concentration of 250 µg mL^{-1} increased the speed of germination in *I. grandifolia*, contrasting with inhibitory effect induced in *D. insularis*. This suggests that other

intrinsic factors may have contributed to the differences between the two species (Mitchell et al., 2017).

Despite the germination processes of *I. grandifolia* being less affected by both treatments when compared with *D. insularis*, the development of their seedlings was inhibited like those of *D. insularis*, suggesting an effective interaction of the active compounds with the seedling tissues. In both weed species, the growth of roots was more strongly inhibited than the aerial parts, possibly due to direct contact of roots with the Bf*Ur* or protodioscin. In the comparison between the potency of Bf*Ur* or protodioscin in each species, protodioscin was in general more active as can be evidenced by the IC_{50} values found for the root growth inhibition. Whereas the IC_{50} of Bf*Ur* was 108 μg mL^{-1} in *D. insularis* and 230 μg mL^{-1} in *I. grandifolia*, the corresponding values for protodioscin were 34 μg mL^{-1} and 54 μg mL^{-1}. In the Bf*Ur*, protodioscin is one of the major substances, but not the only one (Silva, 2012). However, the qualitative similarity of their actions suggested that protodioscin might account for most of the Bf*Ur* action.

The optical microscopy images revealed that the reduction in the primary root length caused by the Bf*Ur* or protodioscin, at their IC_{50} values, in both *D. insularis* and *I. grandifolia* was accompanied by drastic morphological alterations in the root architecture. In both weed species, the primary roots did not expand longitudinally as occurred in the control roots, and in *I. grandifolia*, the lateral roots emerged precociously with both the Bf*Ur* and protodioscin treatments.

Interference with the energy metabolism could be an explanation for the seedling growth reduction, particularly in the root apexes where the tissues require a high metabolic activity for cell division and elongation (Garay-Arroyo et al., 2012). In this respect, by measurements of respiratory activities in root apexes, a significant difference in the respiratory activity of *D. insularis* and *I. grandifolia* roots was observed. In the absence of treatment, the total respiration of *I. grandifolia* roots was significantly lower than that of *D. insularis*. This difference between the two species may be related to the anatomy of roots and/or the presence of cavities in the cortex, possibly aerenchyma structures. The cross-section of the primary roots revealed a higher number of cell layers in *I. grandifolia* when compared with those of the *D. insularis*, a characteristic that would limit the O_2 supply to the internal cells. In general, the aerenchymas are formed to favor the diffusion of O_2 to the cells under hypoxic conditions (Evans, 2004). In fact, it has been demonstrated that a steep concentration gradient across roots exists from the epidermal surface to the cortex. In maize roots, the O_2 concentration is less than half in the center of the stele near the root apex (Ober and Sharp, 1996). Although it is necessary to confirm that the cavities are aerenchymal structures through specific assays (Justin and Armstrong, 1991), the ability of some species of the genus *Ipomoea* to develop lysogenic aerenchymas has been established (Ningsih and Maideliza, 2016).

Because the aerenchymal structures are derived from the death of certain cortical cells which are, therefore, metabolically inactive cells, it seems reasonable to expect that they contributed to lower rates of oxygen consumption that were expressed in the basis of the wet weight of roots. These

structures were also evidenced in the primary roots of *I. grandifolia* treated with either the Bf*Ur* or protodioscin.

In addition to the differences in the respiratory activities of *D. insularis* and *I. grandifolia* roots in untreated conditions, the responses of each weed species to the Bf*Ur* and protodioscin treatments also differed. The COX pathway which represents the mitochondrial oxygen consumption required to meet the energy needs of the cell through ADP oxidative phosphorylation was not significantly altered by both treatments in *D. insularis.* The impairment of energy metabolism it seems, thus, unlikely, a finding that is in agreement with the anatomic images of root cells from *D. insularis* showing that under the Bf*Ur* or protodioscin treatments, despite a root length reduction, the size, format, and organization of the cells were very similar to those of the control.

In *I. grandifolia,* the Bf*Ur* exerted a different effect on the respiration linked to the COX pathway with respect to *D. insularis*: stimulation was observed, most likely reflecting an increase in metabolic activity. Several lateral roots have developed in the whole extent of the primary root, which is an energy-consuming process. As illustrated by the cross-section images of *I. grandifolia* roots treated with the Bf*Ur* and protodioscin (Fig. 9), in eudicots, lateral roots emerge after a repeated periclinal cell division from founder cells and the development of the root meristem, while the xylem and phloem connect to the vasculature in the stele of the parent root (Péret et al., 2009). Different from that found in the Bf*Ur* treatment, protodioscin did not induce similar stimulation in COX-linked respiration, despite also stimulating the development of lateral roots.

Besides the KCN-sensitive respiration, the KCN-insensitive respiration in the root apex of *D. insularis* was also substantially higher than in *I. grandifolia* in the untreated seedlings. Several enzymes contribute to oxygen consumption in KCN-insensitive respiration: the oxygen consumed by the mitochondrial AOX, the extra-mitochondrial oxidases, and the fraction of oxygen converted to oxygen reactive species (ROS). Mitochondria are the main ROS sources during germination and initial seedling growth (Blokhina and Fagerstedt, 2010; Pergo and Ishii-Iwamoto, 2011; Sharma et al., 2012), but under stress conditions, other enzymes also contribute to ROS generation, particularly the NADPH oxidases (EC 1.6.3.1) located in the cell plasma membranes (Tripathy and Oelmüller, 2012). Consistent with high rates of KCN-insensitive respiration of *D. insularis* under untreated conditions, the ROS and MDA content in roots of *D. insularis* was nearly one order of magnitude higher than those of *I. grandifolia*. MDA is one of the lipid peroxidation products that result from the ROS attack on the membrane lipids (Kappus, 1985). The conjugated diene content, which is formed by the reaction of superoxide radicals ($O_2^{\bullet-}$) and peroxyls ($^{\bullet}OH$) on methylene groups of polyunsaturated fatty acids (Smirnoff, 1995), was also higher in *D. insularis* under untreated conditions, but at a lower extent compared with MDA.

Although the Bf*Ur* or protodioscin did not significantly change the KCN-insensitive respiration in both weed species, we cannot discard the possibility that some of the KCN-insensitive processes were altered. For example, the production of ROS by mitochondria or the activity of

NADPH oxidase (Popov et al., 1997; Skutnik and Rychter, 2009). This assumption was supported by the measurements of the ROS and MDA contents.

The ROS content was increased by the protodioscin at the IC_{50} values, in both *D. insularis* and *I. grandifolia* and by the Bf*Ur* in *I. grandifolia.* The relative increment, when compared with their respective untreated seedlings, was substantially higher in *I. grandifolia* than in *D. insularis.* No clear correlation could be identified between the increase in ROS content and the content of MDA and conjugated dienes in *D. insularis* because protodioscin did not change MDA content, and a significant increase was found in the conjugated dienes treated with the Bf*Ur* but not in those treated with protodioscin. Conversely, in *I. grandifolia,* the increase in the ROS content due to both the Bf*Ur* and protodioscin treatments was correlated with an increase in the content of the conjugated diene, while the MDA content decreased. Although these findings suggested that *I. grandifolia* was more susceptible to ROS-induced oxidative damage than *D. insularis,* the increase in ROS content induced by Bf*Ur* or protodioscin treatments in the roots of both weeds may have an additional significance than a condition of cellular oxidative stress.

It has been demonstrated that ROS can act as a critical secondary messenger in the responses of plants to hormones such as IAA, ABA, 24-epibrassinolide, and cytokinins, regulating plant development and also the adaptation to biotic or abiotic stress (Hu et al., 2017; Sharma et al., 2012; Vishwakarma et al., 2017). Further, its role in the differentiation and proliferation of roots has been also demonstrated (Tsukagoshi et al., 2010). Therefore, to exert the signaling responses and avoid the detrimental oxidative damage, the levels of ROS in the plant tissues need to be strictly regulated by a system that comprises several antioxidant enzymes and soluble compounds such as glutathione, ascorbate, and α-tocopherol (Mittler et al., 2011).

Among the soluble antioxidant enzymes, SOD is the first enzyme to eliminate ROS excess, dismuting the superoxide radical ($O_2^{\cdot -}$) into O_2 and hydrogen peroxide (H_2O_2) (Mittler et al., 2011; Scandalios, 1993). The H_2O_2 is subsequently neutralized by the action of other enzymes, including CAT, GR, APX, and POD (Navrot et al., 2007; Sharma et al., 2012). Among these enzymes, the activities of SOD, POD, CAT, and APX were considerably higher in the roots of *D. insularis* than those of *I. grandifolia,* which probably accounts for the neutralization of the high rate of ROS generation in *D. insularis,* under control conditions (Navrot et al., 2007; Sharma et al., 2012). When *D. insularis* were treated with the Bf*Ur* or protodioscin the activities of SOD, APX, CAT, and GR enzymes were not modified, indicating that the antioxidant enzyme system was not activated and therefore, a physiological role for the ROS elevation observed in the protodioscin treatment is a possibility to be considered.

In *I. grandifolia,* the effects of the Bf*Ur* and protodioscin on the antioxidant enzymes were different from those observed in *D. insularis*. Both treatments stimulated the activities of SOD, and protodioscin also activated POD activity. These responses could be interpreted as reactions to minimize the excessive ROS production, which were demonstrated to be relatively higher in *I.*

grandifolia than in *D. insularis* when compared with their respective controls. It should be emphasized, however, that there was a significant reduction in the CAT activity, indicating that the elevation of H_2O_2 may have a role as a signaling mediator in *I. grandifolia* roots in response to Bf*Ur* or protodioscin treatments.

The assumption that the increase in ROS content reflected, at least in part, its action as a signaling mediator, rather than its harmful actions on cell structures was supported by the anatomical and morphological changes observed in the roots of *I. grandifolia* and *D. insularis*. Despite a significant reduction in the primary root length caused by the Bf*Ur* or protodioscin treatments, at their IC_{50} values, there were no typical signs of severe damage to root tissues, such as structural disorganization of the cell layers and the presence of hypertrophic or ruptured cells (Díaz-Tielas et al., 2012; Ishii-Iwamoto et al., 2012). The significant alteration exhibited in the two weeds was the thickening of the cell walls, especially in the more peripheral layers of roots under both treatments.

The most probable explanation for the remarkable shortening of roots in both species is that the Bf*Ur* and protodioscin caused a disturbance in the homeostasis of hormones that act in an integrated way in the initial development of seedlings (Depuydt and Hardtke, 2011; Ubeda-Tomás et al., 2012). A clear reduction in the meristem and the elongation zone of roots along with an early differentiation of tissues was observed as indicated by the development of the lateral roots near the root apexes, the latter phenomenon evident in *I. grandifolia*. The anatomical micrographs performed in the middle region of the *I. grandifolia* roots corroborated this hypothesis, revealing a substantial difference between the vascular cylinders of the control roots and the treatments. Moreover, a region of advanced cellular differentiation of tissues was discernible with an increase in the vascular tissues, which reached a stage where it is already possible to distinguish the presence of the vascular cambium (Fig. 9b, e, h). Such characteristics would not be certainly evidenced in the control seedlings at the middle region of the primary roots, but rather at their upper regions as illustrated by the drawing in Fig. 10.

The treatments also seemed to interfere with the development of the lateral roots since these also exhibited a shortening when compared with the lateral roots of the control (Fig. 7). These morphological changes in the root architecture of *I. grandifolia* are typical responses in seedlings of dicot species submitted to diverse stressors and involving the auxin actions (Laskowski et al., 2006; Potters et al., 2007). Many natural substances that mimic the actions of auxin cause an increase of the primary root length at low concentrations and/or inhibition at higher ones. The stimulation in the development of stems, lateral/adventitious roots and root hairs, along with changes in root gravitropism, are also typically auxin responses (Laskowski et al., 2006; Pacurar et al., 2014). In general, natural compounds mimic or alter the action of IAA by interfering in specific stages of the synthesis, conjugation, transport, signaling, and/or metabolization of the IAA (Cheng et al., 2007). This interference may cause changes in IAA concentration in different zones of the primary root along the longitudinal axis: the meristematic, transition, elongation and/or differentiation zones (Swarup et

al., 2005; Verbelen et al., 2006). An abnormal gradient of IAA concentration in these different areas may positively or negatively affect cell proliferation and morphogenesis of separate cell clusters (Araniti et al., 2017; Cheng et al., 2007) leading, for example, to a precocious stimulation of lateral root development or suppression of the primary root elongation, phenomena that have already been observed in *I. grandifolia* treated with Bf*Ur* or protodioscin.

These morphological alterations have many similarities with phenomena already well described in the literature known as stress-induced morphologic responses (SIMRs). This plant response is triggered by several abiotic-stress such as heavy metals, nutrient deficiency, UV radiation, and hypoxia (Balestri et al., 2014; Potters et al., 2007). According to Potters et al. (2007), the SIMRs are expressed through inhibition of cell elongation, localized stimulation of cell division, and alterations in cell differentiation status. Because the morphogenic responses induced by distinct stresses share common biochemical changes, including ROS production and interferences with auxin actions, it has been suggested that ROS are intermediates between the stress and the development of the SIMR phenotypes (Potters et al., 2007). A link between ROS generation and auxin action in plant response to stress is well documented, although the exact mechanisms are not fully understood (Bielach et al., 2017; KrishnaMurthy and Rathinasabapathi, 2013). It has been suggested that auxins regulate H_2O_2 production by increasing the expression of enzymes that produce superoxides such as NAPDH oxidase and superoxide oxidase (EC 1.10.3.17) and also by reducing the expression of antioxidant enzymes such as catalase and ascorbate oxidase (EC 1.10.3.3) (Iglesias et al., 2010; KrishnaMurthy and Rathinasabapathi, 2013). Moreover, stress can also affect the stability of auxin because the increase in H_2O_2 along with activation of peroxidases promotes the oxidative degradation of IAA (Gazarian et al., 1998).

In agreement with this, besides the characteristic SIMR phenotypes of root systems of *I. grandifolia* in response to the Bf*Ur* and protodioscin treatments, the primary roots presented increased levels of ROS, reduced CAT activity, and increased POD activity. These morphological and biochemical alterations were observed at the IC_{50} doses for primary root growth, which corresponds to sub-lethal doses. In fact, SIMRs typically occur under chronic exposure to sub-lethal doses of the stressor agents to decrease the stress exposure, thereby increasing plant chances to survive. For example, in metal toxicity, the SIMRs are suggested to redirect root development away from a local source of xenobiotics (Potters et al., 2007).

Similar to that found in *I. grandifolia*, some features of an advanced cellular differentiation in the vascular cylinder was also evidenced in *D. insularis*, especially under the But*Ur* treatment, such as the presence of tracheal elements and fibers with thick and lignified cell walls (Dickison, 2000). However, the responses in *D. insularis* roots differed in some aspects from those observed in *I. grandifolia*, possibly due to differences in the morpho-anatomical features of root systems between the mono and dicot species (Osmont et al., 2007). In monocots, lateral roots usually do not develop from the primary root. Rather, at the initial stage of seedling development, the adventitious roots are

represented by nodal or seminal roots as reported by Verdú and Mas (2014) in *Digitaria sanguinalis.* Different from those found in *I. grandifolia*, the responses of *D. insularis* to the Bf*Ur* and protodioscin treatments were not characteristics of SIMRs. Both treatments reduced the elongation of the primary roots but did not increase the number of adventitious roots in *D. insularis* (Fig. 6). Although auxins also regulate the development of adventitious roots in monocots (Pacurar et al., 2014), in *D. insularis*, its action was apparently impaired in treated seedlings. In agreement with this assumption, there was a decrease in root hairs, whose formation has been demonstrated to be intensified by auxin and ethylene (Hu et al., 2017; Zhang et al., 2016). It seems plausible to suggest that, due to the higher susceptibility of *D. insularis* roots to active components of the Bf*Ur* and protodioscin (lower IC_{50}), the reduction in the number of root hairs represents a defensive response to minimize the absorption of toxicants.

The alterations observed in both the epidermis and exodermis of the primary roots of both *D. insularis* and *I. grandifolia* treated with the Bf*Ur* or protodioscin could represent another mechanism for reducing the access of toxic compounds to the internal structures of roots. The cross-section images revealed irregular cell shapes together with thickening of the cell walls (Figs. 8f, i, 9f, i), possibly due to an increased deposition of polymers like suberin and lignin in the cell walls (Baxter et al., 2009). This phenomenon has demonstrated to alter the apoplastic flow of organic xenobiotic and also of inorganic compounds and ions (Wild et al., 2005). The lignification in exoderm, sclerenchyma, and root endodermis is linked to an increase in ROS and POD activity (Bouranis et al., 2003), alterations that were observed in the primary roots of *I. grandifolia* treated with the Bf*Ur* or protodioscin.

The irregularities observed in the epidermis and exodermis cells may also be the consequences of the accumulation of protodioscin and other chemical constituents of the Bf*Ur* in the cell wall, a phenomenon that has been observed in the protection against other xenobiotics such as cadmium (Khan et al., 1984) and lead (Phang et al., 2011). Protodioscin consists of a combination of hydrophilic sugars with a furostanol-type steroidal group, which confers the amphiphilic character typical of most saponins. This property also favors the interaction of protodioscin with the bilayer lipid structure and its binding with the membrane macromolecules, especially sterols and phospholipids (Lorent et al., 2014; Steel and Drysdale, 1988). The most known consequences of this interaction are the rupture of erythrocyte membranes (hemolysis) (Voutquenne et al., 2002) and the fungicidal effects resulting from the interaction with ergosterol in levedures (Armah et al., 1999; Polacheck et al., 1991).

The interaction of protodioscin and other components of the Bf*Ur* with membrane phytosterols likely affected the integrity of the plasmatic membranes of the external cells. These findings suggest that the changes in ionic permeability caused by the Bf*Ur* and protodioscin in the roots of *I. grandifolia* and *D. insularis* could be the result of increased permeability of the plasma membranes to ions and/or reduced apoplastic inflow of ions due to thickening of cell walls.

Further evidence of the direct interaction of the Bf*Ur* components with the membranes was provided by the primary root browning observed in both weed species. The enzymatic browning of

different plant tissues is another consequence of ROS-induced attack on cellular membranes (Cheng et al., 2015). The disruption of membrane integrity activates the polyphenol oxidase (PPO; EC 1.10.3.1, 1.10.3.2 and/or 1.14.18.1) that utilizes polyphenol compounds located inside vacuoles as substrates for the production of brown substances (Chikezie et al., 2013).

It was remarkable that the Bf*Ur* and protodioscin at their respective IC_{50} values induced, in general, similar alterations in all the assayed parameters in each species, irrespective of some distinct effects evidenced in the root morphology and the biochemical responses in *D. insularis* and *I. grandifolia.* This observation confirms our previous assumption that protodioscin and its isomers accounted for most of the activity of the Bf*Ur*, with other components being less active.

In summary, most of the biochemical, morpho-anatomical, and cytological alterations found in *D. insularis* and *I. grandifolia* in response to the Bf*Ur* or protodioscin treatment at their IC_{50} values seem to reflect plant adaptive strategies to survive in the presence of toxicants. It seems plausible to suggest that the direct interaction of protodioscin with external cells initiates a stress response mediated by ROS production, thereby triggering the subsequent defensive responses that include the activation of antioxidant defense systems and anatomical and morphological changes in the root architecture mediated by the hormones, especially auxins. Conversely, the eudicot weed *I. grandifolia* was shown to be more tolerant to the Bf*Ur* and protodioscin as indicated by the higher IC_{50} values compared to *D. insularis*. Despite this, *I. grandifolia* exhibited ROS-induced peroxidative damage in its roots and inhibition of the germination processes. In *D. insularis,* besides lack of effect on the seed germination, no root oxidative damage was observed, possibly to its higher capacity of antioxidant defense system to cope with stress compared to that of *I. grandifolia*.

At concentrations higher than their IC_{50} values, the Bf*Ur* and protodioscin treatments induced a progressive decrease in the growth in both weed seedlings, as shown in Fig. 2, suggesting that the adaptive strategies and the protective defense mechanism could be no longer effective to avoid oxidative damage due to excessive ROS generation.

Overall, it can be concluded that, despite species-specific differences in sensitivity and mode of action on weeds, the *U. ruziziensis* mulches can reduce weed emergence in the field through chemical effects when applied at adequate doses, with the saponin protodioscin being one of its phytotoxic components. The relevance of findings in this work may lead to more efficient no-tillage crop rotations including *U. ruziziensis*. Ultimately, such findings may contribute to the use of natural and renewable weed control tools.

Funding

This work was supported by grants from the Araucária Foundation for Scientific and Technological Development of Paraná State (FA-112/2010) and National Council for Scientific and Technological

Development (CNPq - 308980/2017-4). Paulo Vinicius Moreira da Costa Menezes received a scholarship from the Coordination for the Improvement of Higher Education Personnel (CAPES).

REFERENCES

Aebi, H., 1984. [13] Catalase in Vitro. Methods Enzymol. 105, 121–126. https://doi.org/10.1016/S0076-6879(84)05016-3

Araniti, F., Bruno, L., Sunseri, F., Pacenza, M., Forgione, I., Bitonti, M.B., Abenavoli, M.R., 2017. The allelochemical farnesene affects *Arabidopsis thaliana* root meristem altering auxin distribution. Plant Physiol. Biochem. 121, 14–20. https://doi.org/10.1016/j.plaphy.2017.10.005

Armah, C.N., Mackie, A.R., Roy, C., Price, K., Osbourn, A.E., Bowyer, P., Ladha, S., 1999. The membrane-permeabilizing effect of avenacin A-1 involves the reorganization of bilayer cholesterol. Biophys. J. 76, 281–290. https://doi.org/10.1016/S0006-3495(99)77196-1

Balestri, M., Ceccarini, A., Forino, L.M.C., Zelko, I., Martinka, M., Lux, A., Ruffini Castiglione, M., 2014. Cadmium uptake, localization and stress-induced morphogenic response in the fern *Pteris vittata*. Planta 239, 1055–1064. https://doi.org/10.1007/s00425-014-2036-z

Baxter, I., Hosmani, P.S., Rus, A., Lahner, B., Borevitz, J.O., Muthukumar, B., Mickelbart, M. V., Schreiber, L., Franke, R.B., Salt, D.E., 2009. Root suberin forms an extracellular barrier that affects water relations and mineral nutrition in *Arabidopsis* . PLoS Genet. 5. https://doi.org/10.1371/journal.pgen.1000492

Bielach, A., Hrtyan, M., Tognetti, V.B., 2017. Plants under stress: Involvement of auxin and cytokinin. Int. J. Mol. Sci. 18, 1427. https://doi.org/10.3390/ijms18071427

Blokhina, O., Fagerstedt, K.V., 2010. Reactive oxygen species and nitric oxide in plant mitochondria: Origin and redundant regulatory systems. Physiol. Plant. 138, 447–462. https://doi.org/10.1111/j.1399-3054.2009.01340.x

Bouranis, D.L., Chorianopoulou, S.N., Siyiannis, V.F., Protonotarios, V.E., Hawkesford, M.J., 2003. Aerenchyma formation in roots of maize during sulphate starvation. Planta 217, 382–391. https://doi.org/10.1007/s00425-003-1007-6

Boveris, A., Sanchez, R.A., Varsavsky, A.I., 1980. Chemiluminescence measurements. FEBS Lett. 113, 29–32.

Bradford, M.M., 1976. A rapid and sensitive method for the quantitation of microgram quantities of protein utilizing the principle of protein-dye binding. Anal. Biochem. 72, 248–254. https://doi.org/10.1016/0003-2697(76)90527-3

Brum, K.B., Haraguchi, M., Garutti, M.B., Nóbrega, F.N., Rosa, B., Fioravanti, M.C.S., 2009. Steroidal saponin concentrations in *Brachiaria decumbens* and *B. brizantha* at different developmental stages. Cienc. Rural 39, 279–281. https://doi.org/10.1590/S0103-84782008005000034

Carvalho, L.B., Cruz-Hipolito, H., González-Torralva, F., da Costa Aguiar Alves, P.L.,

Christoffoleti, P.J., De Prado, R., 2011. Detection of Sourgrass (*Digitaria insularis*) biotypes resistant to glyphosate in Brazil. Weed Sci. 59, 171–176. https://doi.org/10.1614/ws-d-10-00113.1

Carvalho, S.J.P., Nicolai, M., Ferreira, R.R., De Oliveira Figueira, A.V., Christoffoleti, P.J., 2009. Herbicide selectivity by differential metabolism: Considerations for reducing crop damages. Sci. Agric. 66, 136–142. https://doi.org/10.1590/s0103-90162009000100020

Cheng, Y., Liu, L., Zhao, G., Shen, C., Yan, H., Guan, J., Yang, K., 2015. The effects of modified atmosphere packaging on core browning and the expression patterns of PPO and PAL genes in "Yali" pears during cold storage. LWT - Food Sci. Technol. 60, 1243–1248. https://doi.org/10.1016/j.lwt.2014.09.005

Cheng, Y., Qin, G., Dai, X., Zhao, Y., 2007. NPY1, a BTB-NPH3-like protein, plays a critical role in auxin-regulated organogenesis in *Arabidopsis*. Proc. Natl. Acad. Sci. U. S. A. 104, 18825–18829. https://doi.org/10.1073/pnas.0708506104

Chiapusio, G., Sánchez, A.M., Reigosa, M.J., González, L., Pellissier, F., 1997. Do germination indices adequately reflect allelochemical effects on the germination process? J. Chem. Ecol. 23, 2445–2453. https://doi.org/10.1023/B:JOEC.0000006658.27633.15

Chikezie, P.C., Akuwudike, A.R., Chikezie, C.M., Ibegbulem, C.O., 2013. Fractional purification and kinetic parameters (K_m and Vmax) of polyphenol oxidase extracted from three segments of *Solanum melongenas* and *Musa sapientum* fruits. Am. J. Plant Physiol. 8, 84–92. https://doi.org/10.3923/ajpp.2013.84.92

Depuydt, S., Hardtke, C.S., 2011. Hormone signalling crosstalk in plant growth regulation. Curr. Biol. 21, R365–R373. https://doi.org/10.1016/j.cub.2011.03.013

Díaz-Tielas, C., Graña, E., Sotelo, T., Reigosa, M.J., Sánchez-Moreiras, A.M., 2012. The natural compound trans-chalcone induces programmed cell death in *Arabidopsis thaliana* roots. Plant, Cell Environ. 35, 1500–1517. https://doi.org/10.1111/j.1365-3040.2012.02506.x

Dickison, W.C., 2000. Integrative plant anatomy. Hartcourt Academic Press, 533.

Evans, D.E., 2004. Aerenchyma formation. New Phytol. 161, 35–49. https://doi.org/10.1046/j.1469-8137.2003.00907.x

Foletto, M.P., Kagami, F., Voll, E., Kern-Cardoso, K.A., Pergo-Coelho, E.M., Rocha, M., Silva, A.A., Sarragiotto, M.H., Ishii-Iwamoto, E.L., 2012. Allelopathic effects of *Brachiaria ruziziensis* and aconitic acid on *Ipomoea triloba* weed. Allelopath. J. 30, 33–48.

Foyer, C.H., Halliwell, B., 1976. The presence of glutathione and glutathione reductase in chloroplasts: A proposed role in ascorbic acid metabolism. Planta 133, 21–25. https://doi.org/10.1007/BF00386001

Furlan, F.H., Colodel, E.M., Lemos, R.A.A., Castro, M.B., Mendoça, F.S., Riet-Correa, F., 2012. Poisonous plant affecting cattle in Central-Western Brazil. Int. J. Poisonous Plant Res. 2, 1–13.

Garay-Arroyo, A., De La Paz Sánchez, M., García-Ponce, B., Azpeitia, E., Álvarez-Buylla, E.R., 2012. Hormone symphony during root growth and development. Dev. Dyn. 241, 1867–1885.

https://doi.org/10.1002/dvdy.23878

Gazarian, I.G., Lagrimini, L.M., Mellon, F.A., Naldrett, M.J., Ashby, G.A., Thorneley, R.N.F., 1998. Catalysed oxidation of Indol-3-Yl acetic acid. Biochem. J. 232, 223–232.

Giannopolitis, C.N., Ries, S.K., 1977. Superoxide dismutases: I. Occurrence in higher plants. Plant Physiol. 59, 309–14. https://doi.org/10.1104/pp.59.2.309

Heath, R.L., Packer, L., 1968. Photoperoxidation in isolated chloroplasts. Arch. Biochem. Biophys. 125, 189–198. https://doi.org/10.1016/0003-9861(68)90654-1

Hoagland, R.E., Zablotowicz, R.M., Reddy, K.N., 1996. Studies of the phytotoxicity of saponins on weed and crop plants. Adv. Exp. Med. Biol. 405, 57–73. https://doi.org/10.1007/978-1-4613-0413-5_6

Hu, Y., Vandenbussche, F., Van Der Straeten, D., 2017. Regulation of seedling growth by ethylene and the ethylene–auxin crosstalk. Planta 245, 467–489. https://doi.org/10.1007/s00425-017-2651-6

Hussain, M., Debnath, B., Qasim, M., Steve Bamisile, B., Islam, W., Hameed, M.S., Wang, L., Qiu, D., 2019. Role of saponins in plant defense against specialist herbivores. Molecules 24, 1–21. https://doi.org/10.3390/molecules24112067

Iglesias, M.J., Terrile, M.C., Bartoli, C.G., D'Ippólito, S., Casalongué, C.A., 2010. Auxin signaling participates in the adaptative response against oxidative stress and salinity by interacting with redox metabolism in *Arabidopsis*. Plant Mol. Biol. 74, 215–222. https://doi.org/10.1007/s11103-010-9667-7

Ishii-Iwamoto, E.L., Abrahim, D., Sert, M.A., Bonato, C.M., Kelmer-Bracht, A.M., Bracht, A., 2006. Mitochondria as a site of allelochemical action. Allelopath. A Physiol. Process with Ecol. Implic. 105, 267–284. https://doi.org/10.1007/1-4020-4280-9_12

Ishii-Iwamoto, E.L., Pergo-Coelho, E.M., Reis, B., Moscheta, I.S., Bonato, C.M., 2012. Effects of monoterpenes on physiological processes during seed germination and seedling growth. Curr. Bioact. Compd. 8, 50–64. https://doi.org/10.2174/157340712799828223

Jambunathan, N., 2010. Plant Stress Tolerance. NIH Public Access 639, 1–14. https://doi.org/10.1007/978-1-60761-702-0

Justin, S.H.F.W., Armstrong, W., 1991. Evidence for the involvement of ethene in aerenchyma formation in adventitious roots of rice (*Oryza sativa* L.). New Phytol. 118, 49–62. https://doi.org/10.1111/j.1469-8137.1991.tb00564.x

Kappus, H., 1985. Lipid peroxidation: mechanisms, analysis, enzymology and biological relevance. Oxidative Stress 273.

Kelley, K.B., Riechers, D.E., 2007. Recent developments in auxin biology and new opportunities for auxinic herbicide research. Pestic. Biochem. Physiol. 89, 1–11. https://doi.org/10.1016/j.pestbp.2007.04.002

Khan, D.H., Duckett, J.G., Frankland, B., Brian Kirkham, J., 1984. An X-ray microanalytical

study of the distribution of Cadmium in roots of *Zea mays* L. J. Plant Physiol. 115, 19–28. https://doi.org/10.1016/S0176-1617(84)80047-4

KrishnaMurthy, A., Rathinasabapathi, B., 2013. Oxidative stress tolerance in plants: Novel interplay between auxin and reactive oxygen species signaling. Plant Signal. Behav. 8, 1–5. https://doi.org/10.4161/psb.25761

Labouriau, L.G., Osborn, J.H., 1984. Temperature dependence of the germination of tomato seeds. J. Therm. Biol. 9, 285–294. https://doi.org/10.1016/0306-4565(84)90010-X

Laskowski, M., Biller, S., Stanley, K., Kajstura, T., Prusty, R., 2006. Expression profiling of auxin-treated *Arabidopsis* roots: Toward a molecular analysis of lateral root emergence. Plant Cell Physiol. 47, 788–792. https://doi.org/10.1093/pcp/pcj043

Lorent, J.H., Quetin-Leclercq, J., Mingeot-Leclercq, M.P., 2014. The amphiphilic nature of saponins and their effects on artificial and biological membranes and potential consequences for red blood and cancer cells. Org. Biomol. Chem. 12, 8803–8822. https://doi.org/10.1039/c4ob01652a

Lozano, M.C., Martinez, N.M., Diaz, G.J., 2017. Content of the saponin protodioscin in *Brachiaria* spp. from the eastern plains of Colombia. Toxins (Basel). 9, 1–12. https://doi.org/10.3390/toxins9070220

Mert-Türk, F., 2006. Saponins versus plant fungal pathogens. J. Cell Mol. Biol. 5, 13–17.

Mitchell, J., Johnston, I.G., Bassel, G.W., 2017. Variability in seeds: Biological, ecological, and agricultural implications. J. Exp. Bot. 68, 809–817. https://doi.org/10.1093/jxb/erw397

Mito, M.S., Silva, A.A., Kagami, F.L., Almeida, J.D., Mantovanelli, G.C., Barbosa, M.C., Kern-Cardoso, K.A., Ishii-Iwamoto, E.L., 2019. Responses of the weed *Bidens pilosa* L. to exogenous application of the steroidal saponin protodioscin and plant growth regulators 24-epibrassinolide, indol-3-acetic acid and abscisic acid. Plant Biol. 21, 326–335. https://doi.org/10.1111/plb.12927

Mittler, R., Vanderauwera, S., Suzuki, N., Miller, G., Tognetti, V.B., Vandepoele, K., Gollery, M., Shulaev, V., Van Breusegem, F., 2011. ROS signaling: The new wave? Trends Plant Sci. 16, 300–309. https://doi.org/10.1016/j.tplants.2011.03.007

Müller, M., Schmidt, W., 2004. Environmentally induced plasticity of root hair development in *Arabidopsis*. Plant Physiol. 134, 409–419. https://doi.org/10.1104/pp.103.029066

Nakano, Y., Asada, K., 1981. Hydrogen peroxide is scavenged by Ascorbate-specific peroxidase in Spinach chloroplasts. Plant Cell Physiol. 22, 867–880.

Navrot, N., Rouhier, N., Gelhaye, E., Jacquot, J.P., 2007. Reactive oxygen species generation and antioxidant systems in plant mitochondria. Physiol. Plant. 129, 185–195. https://doi.org/10.1111/j.1399-3054.2006.00777.x

Nepomuceno, M., Chinchilla, N., Varela, R.M., Molinillo, J.M.G., Lacret, R., Alves, P.L.C.A., Macias, F.A., 2017. Chemical evidence for the effect of *Urochloa ruziziensis* on glyphosate-resistant soybeans. Pest Manag. Sci. 73, 2071–2078. https://doi.org/10.1002/ps.4578

Ningsih, A., Maideliza, T., 2016. The growth of aerenchyma of Terrestrial Kale (*Ipomoea*

reptans Poir) and Water Kale (*Ipomoea aquatic* Forsk). Al-Kauniyah J. Biol. 9, 37–43.

O'Brien, T.P., Feder, N., McCully, M.E., 1964. Polychromatic staining of plant cell walls by toluidine blue O. Protoplasma 59, 368–373. https://doi.org/10.1007/BF01248568

Ober, E.S., Sharp, R.E., 1996. A microsensor for direct measurement of O_2 partial pressure within plant tissues. J. Exp. Bot. 47, 447–454. https://doi.org/10.1093/jxb/47.3.447

Oliveira Jr, R.S., Rios, F.A., Constantin, J., Ishii-Iwamoto, E.L., Gemelli, A., Martini, P.E., 2014. Grass straw mulching to suppress emergence and early growth of weeds. Planta Daninha 32, 11–17. https://doi.org/10.1590/s0100-83582014000100002

Osmont, K.S., Sibout, R., Hardtke, C.S., 2007. Hidden branches: Developments in root system architecture. Annu. Rev. Plant Biol. 58, 93–113. https://doi.org/10.1146/annurev.arplant.58.032806.104006

Pacurar, D.I., Perrone, I., Bellini, C., 2014. Auxin is a central player in the hormone cross-talks that control adventitious rooting. Physiol. Plant. 151, 83–96. https://doi.org/10.1111/ppl.12171

Pazuch, D., Trezzi, M.M., Guimarães, A.C.D., Barancelli, M.V.J., Pasini, R., Vidal, R.A., 2017. Evolution of natural resistance to glyphosate in Morning Glory populations. Planta Daninha 35. https://doi.org/10.1590/s0100-83582017350100009

Péret, B., De Rybel, B., Casimiro, I., Benková, E., Swarup, R., Laplaze, L., Beeckman, T., Bennett, M.J., 2009. *Arabidopsis* lateral root development: an emerging story. Trends Plant Sci. 14, 399–408. https://doi.org/10.1016/j.tplants.2009.05.002

Pergo, E.M., Ishii-Iwamoto, E.L., 2011. Changes in energy metabolism and antioxidant defense systems during seed germination of the weed species *Ipomoea triloba* L. and the responses to allelochemicals. J. Chem. Ecol. 37, 500–513. https://doi.org/10.1007/s10886-011-9945-0

Phang, I.C., Leung, D.W.M., Taylor, H.H., Burritt, D.J., 2011. Correlation of growth inhibition with accumulation of Pb in cell wall and changes in response to oxidative stress in *Arabidopsis thaliana* seedlings. Plant Growth Regul. 64, 17–25. https://doi.org/10.1007/s10725-010-9527-0

Podolak, I., Galanty, A., Sobolewska, D., 2010. Saponins as cytotoxic agents: A review. Phytochem. Rev. 9, 425–474. https://doi.org/10.1007/s11101-010-9183-z

Polacheck, I., Levy, M., Guizie, M., Zehavi, U., Naim, M., Evron, R., 1991. Mode of action of the antimycotic agent G2 isolated from Alfalfa roots. Zentralblatt fur Bakteriol. 275, 504–512. https://doi.org/10.1016/S0934-8840(11)80172-6

Popov, V.N., Simonian, R.A., Skulachev, V.P., Starkov, A.A., 1997. Inhibition of the alternative oxidase stimulates H_2O_2 production in plant mitochondria. FEBS Lett. 415, 87–90. https://doi.org/10.1016/S0014-5793(97)01099-5

Potters, G., Pasternak, T.P., Guisez, Y., Palme, K.J., Jansen, M.A.K., 2007. Stress-induced morphogenic responses: growing out of trouble? Trends Plant Sci. 12, 98–105. https://doi.org/10.1016/j.tplants.2007.01.004

Pütter, J., 1974. Peroxidases. Methods Enzym. Anal. 685–690. https://doi.org/10.1016/b978-0-12-091302-2.50033-5

Recknagel, R.O., Glende, E.A., 1984. Spectrophotometric detection of lipid conjugated dienes. Methods Enzymol. 105, 331–337. https://doi.org/10.1016/S0076-6879(84)05043-6

Sánchez-Moreiras, A.M., Reigosa, M.J., 2018. Advances in Plant Ecophysiology Techniques. Springer International Publishing.

São Miguel, A.S.D.C., Pacheco, L.P., Souza, E.D., Silva, C.M.R., Carvalho, C., 2018. Cover crops in the weed management in soybean culture. Planta Daninha 36, 1–10. https://doi.org/10.1590/S0100-83582018360100072

Scandalios, J.G., 1993. Oxygen stress and superoxide dismutases. Plant Physiol. 101, 7–12. https://doi.org/10.1104/pp.101.1.7

Sharma, P., Jha, A.B., Dubey, R.S., Pessarakli, M., 2012. Reactive oxygen species, oxidative damage, and antioxidative defense mechanism in plants under stressful conditions. J. Bot. 2012, 1–26. https://doi.org/10.1155/2012/217037

Silva, A.A., 2012. Evaluation of allelopathic effects and isolation of constituents of the active fractions of the species *Brachiaria ruziziensis* and *Pennisetum glaucum* (*Poaceae*) (Thesis, 115 pp, BCE-UEM S586aTe/Pc633.2). State University of Maringá.

Skutnik, M., Rychter, A.M., 2009. Differential response of antioxidant systems in leaves and roots of barley subjected to anoxia and post-anoxia. J. Plant Physiol. 166, 926–937. https://doi.org/10.1016/j.jplph.2008.11.010

Smirnoff, N., 1995. Environment and plant metabolism: flexibility and acclimation. Choice Rev. Online 33, 33-0308-33–0308. https://doi.org/10.5860/choice.33-0308

Steel, C.C., Drysdale, R.B., 1988. Electrolyte leakage from plant and fungal tissues and disruption of liposome membranes by α-tomatine. Phytochemistry 27, 1025–1030. https://doi.org/10.1016/0031-9422(88)80266-8

Sterling, T.M., 1997. Mechanism of action of natural auxins and the auxinic herbicides. Rev. Toxicol. 1, 111–141.

Swarup, R., Kramer, E.M., Perry, P., Knox, K., Leyser, H.M.O., Haseloff, J., Beemster, G.T.S., Bhalerao, R., Bennett, M.J., 2005. Root gravitropism requires lateral root cap and epidermal cells for transport and response to a mobile auxin signal. Nat. Cell Biol. 7, 1057–1065. https://doi.org/10.1038/ncb1316

Tripathy, B.C., Oelmüller, R., 2012. Reactive oxygen species generation and signaling in plants. Plant Signal. Behav. 7, 37–41. https://doi.org/10.4161/psb.22455

Tsukagoshi, H., Busch, W., Benfey, P.N., 2010. Transcriptional regulation of ROS controls transition from proliferation to differentiation in the root. Cell 143, 606–616. https://doi.org/10.1016/j.cell.2010.10.020

Tsurumi, S., Ishizawa, K., Rahman, A., Soga, K., Hoson, T., Goto, N., Kamisaka, S., 2000.

Effects of chromosaponin I and brassinolide on the growth of roots in etiolated *Arabidopsis* seedlings. J. Plant Physiol. 156, 60–67. https://doi.org/10.1016/S0176-1617(00)80273-4

Ubeda-Tomás, S., Beemster, G.T.S., Bennett, M.J., 2012. Hormonal regulation of root growth: Integrating local activities into global behaviour. Trends Plant Sci. 17, 326–331. https://doi.org/10.1016/j.tplants.2012.02.002

Vanlerberghe, G.C., 2013. Alternative oxidase: A mitochondrial respiratory pathway to maintain metabolic and signaling homeostasis during abiotic and biotic stress in plants. Int. J. Mol. Sci. 14, 6805–6847. https://doi.org/10.3390/ijms14046805

Verbelen, J.P., De Cnodder, T., Le, J., Vissenberg, K., Baluška, F., 2006. The root apex of *Arabidopsis thaliana* consists of four distinct zones of growth activities: Meristematic zone, transition zone, fast elongation zone and growth terminating zone. Plant Signal. Behav. 1, 296–304. https://doi.org/10.4161/psb.1.6.3511

Verdú, A.M.C., Mas, M.T., 2014. *Digitaria sanguinalis* seedling development pattern: Relationship with seed origin. Plant Biosyst. 148, 42–48. https://doi.org/10.1080/11263504.2012.755135

Vishwakarma, K., Upadhyay, N., Kumar, N., Yadav, G., Singh, J., Mishra, R.K., Kumar, V., Verma, R., Upadhyay, R.G., Pandey, M., Sharma, S., 2017. Abscisic acid signaling and abiotic stress tolerance in plants: A review on current knowledge and future prospects. Front. Plant Sci. 8, 1–12. https://doi.org/10.3389/fpls.2017.00161

Voutquenne, L., Lavaud, C., Massiot, G., Le Men-Olivier, L., 2002. Structure-activity relationships of haemolytic saponins. Pharm. Biol. 40, 253–262. https://doi.org/10.1076/phbi.40.4.253.8470

Wild, E., Dent, J., Thomas, G.O., Jones, K.C., 2005. Direct observation of organic contaminant uptake, storage, and metabolism within plant roots. Environ. Sci. Technol. 39, 3695–3702. https://doi.org/10.1021/es048136a

Zhang, D., Xia, R., Cao, X., 2016. Ethylene modulates root hair development in trifoliate orange through auxin-signaling pathway. Sci. Hortic. (Amsterdam). 213, 252–259. https://doi.org/10.1016/j.scienta.2016.11.007

SUPPLEMENTARY MATERIAL

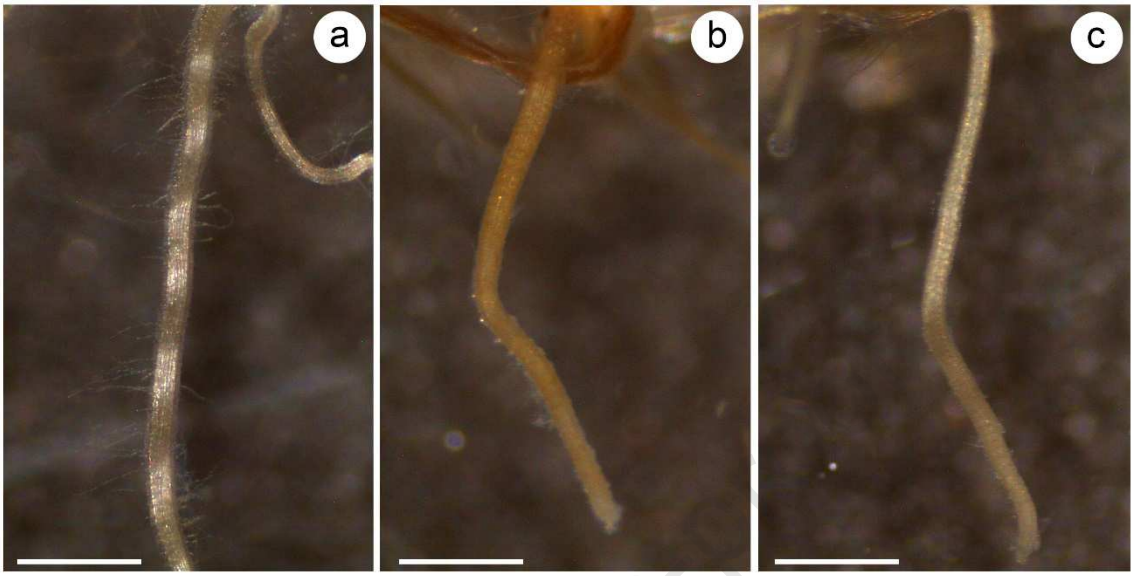

Figure 1S – Root morphology of *D. insularis* treated for 120 hours, detaching the presence (control) or absence (treatments) of root hairs. The concentrations of Bf*Ur* and protodioscin were the IC_{50} values 108 and 34 µg mL^{-1}, respectively. Control (a); Bf*Ur* (b), protodioscin (c). Scale: (a, b, c)—1 mm.

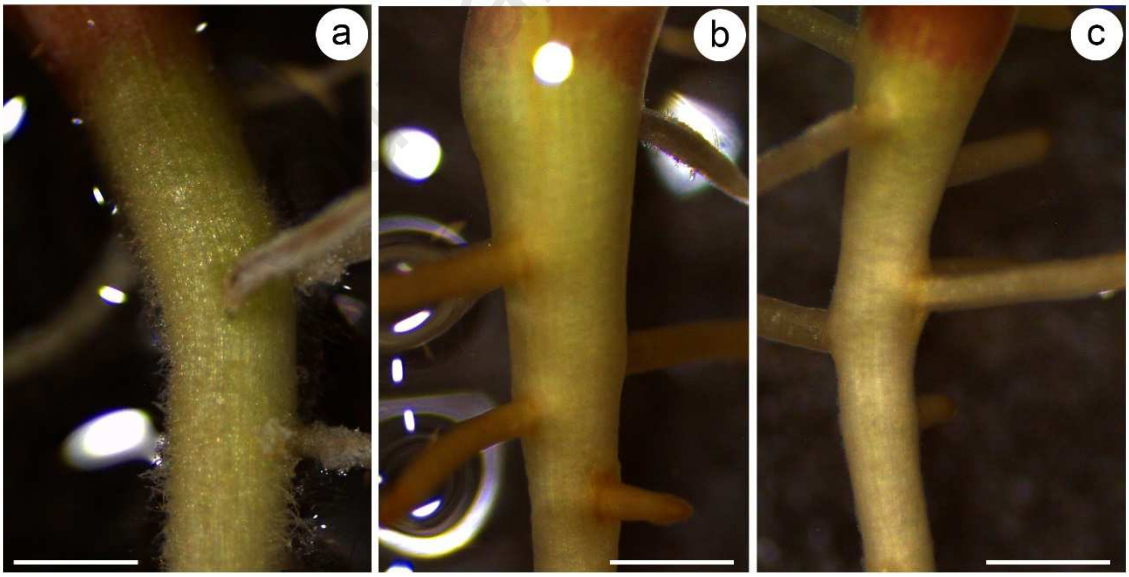

Figure 2S – Root morphology of *I. grandifolia* treated for 120 hours, detaching the presence (control) or absence (treatments) of root hairs. The concentrations of Bf*Ur* and protodioscin were the IC_{50} values 230 and 54 µg mL^{-1}, respectively. Control (a); Bf*Ur* (b), protodioscin (c). Scale: (a, b, c)—1 mm

Highlights

Urochloa ruziziensis extract and protodioscin induce morphogenic responses in weeds

Urochloa ruziziensis inhibits *Digitaria insularis* and *Ipomoea grandifolia* growth

Urochloa ruziziensis compounds induce ROS-induced peroxidative damage in weeds

DECLARATION OF INTERESTS

The authors declare that they have no known competing financial interests or personal relationships that could have appeared to influence the work reported in this paper